Food Chemistry: X 12 (2021) 100168

Contents lists available at ScienceDirect

Food Chemistry: X

journal homepage: www.sciencedirect.com/journal/food-chemistry-x

Applications of infrared spectroscopy in polysaccharide structural analysis: Progress, challenge and perspective

Tao Hong, Jun-Yi Yin *, Shao-Ping Nie, Ming-Yong Xie *

State Key Laboratory of Food Science and Technology, China-Canada Joint Laboratory of Food Science and Technology (Nanchang), Nanchang University, 235 Nanjing East Road, Nanchang, Jiangxi 330047, People's Republic of China

ARTICLE INFO

Keywords:
Polysaccharide structure
IR spectroscopy
IRMPD
Cryogenic IR-MS
IR imaging
DFT

ABSTRACT

Polysaccharides are important biomacromolecules with numerous beneficial functions and a wide range of industrial applications. Functions and properties of polysaccharides are closely related to their structural features. Infrared (IR) spectroscopy is a well-established technique which has been widely applied in polysaccharide structural analysis. In this paper, the principle of IR and interpretation of polysaccharide IR spectrum are briefly introduced. Classical applications of IR spectroscopy in polysaccharide structural elucidation are reviewed from qualitative and quantitative aspects. Some advanced IR techniques including integrating with mass spectrometry (MS), microscopy and computational chemistry are introduced and their applications are emphasized. These emerging techniques can considerably expand application scope of IR, thus exert a more important effect on carbohydrate characterization. Overall, this review seeks to provide a comprehensive insight to applications of IR spectroscopy in polysaccharide structural analysis and highlights the importance of advanced IR-integrating techniques.

Introduction

Polysaccharides are polymeric carbohydrate macromolecules in which monosaccharide units are covalently linked by glycosidic bonds, in either a linear or branched configuration. Like other biological macromolecules such as nucleic acids and proteins, polysaccharides are ubiquitous in almost all life forms in nature, and play essential roles in the existence and living activities of all known organisms (Barbosa & de Carvalho Junior, 2021). In addition, owing to their outstanding structure features and functional properties, polysaccharides have been widely used in pharmaceutical (Arlov, Rutsche, Korayem, Ozturk, & Zenobi-Wong, 2021), environmental (Nasrollahzadeh, Sajjadi, Iravani, & Varma, 2021) and food industries (Cui et al., 2021).

Polysaccharide structural information is the theoretical foundation of understanding polysaccharide structure–function relationship. Compared with other biological macromolecules, structure of polysaccharide is much more complex due to the diversity of monomeric units and linkage types (Ray, Schutz, Mukherjee, Jana, Ray, & Marschall, 2021). On account of this structural complexity, research in polysaccharides has lagged far behind nucleic acids and proteins. Hence, polysaccharide structure analysis is an important but challenging task. Different analytical techniques including spectral, chemical and chromatographic analysis, are applied for the elucidation of the fine chemical structure of polysaccharides.

Infrared (IR) spectroscopy is a rapid, nondestructive and accessible spectral technique, which has been widely applied in polysaccharide structure analysis. Applications of IR spectroscopy in this field have been reviewed by several researchers. For example, IR spectra of 14 carbohydrates were collected and their spectra features were given in detail by Wiercigroch et al. (2017). Applications of IR spectroscopic methods in cellulose analysis in both isolated state and plant cell wall (PCW) were discussed by Makarem et al. (2019). There were also some reviews about IR imaging of polysaccharides in PCW (Gierlinger, 2018; Kumar, Lahlali, Liu, & Karunakaran, 2016; Wu, Huang, Chen, Chen, & Liu, 2019). However, these papers are more specific to only one application filed rather than comprehensive. Hence, to acknowledge recent development and grasp the future trends in the application of IR spectroscopy in polysaccharide structure analysis, a comprehensive review is greatly needed.

This review begins with a berif introduction of principle of IR spectroscopy and interpretation of polysaccharide IR spectrum. Then, some classical applications of IR spectroscopy in polysaccharide elucidation

* Corresponding authors.
E-mail addresses: yinjy@ncu.edu.cn (J.-Y. Yin), myxie@ncu.edu.cn (M.-Y. Xie).

https://doi.org/10.1016/j.fochx.2021.100168
Received 7 October 2021; Received in revised form 16 November 2021; Accepted 19 November 2021
Available online 20 November 2021

are discussed from qualitative and quantitative aspects. Lastly, some advanced IR techniques such as integrating with mass spectrometry (MS), microscopy and computational chemistry are introduced.

Principle and spectrum interpretation

Principle of IR spectroscopy

IR spectroscopy is an extensively applied analytical technique for molecular structural studies. IR light can be divided into three subregions, far-IR (FIR), mid-IR (MIR) and near-IR (NIR). Among these subregions, MIR region of the electromagnetic spectrum lies in wavelength between 2500 nm and 25000 nm (wavenumber between 4000 cm^{-1} to 400 cm^{-1}). It is typically applied to molecular structure determination and confirmation of organic compounds. Because the frequencies of radiations in this region matches in energy with natural vibrational frequencies of bonds in organic molecules. An IR spectrum is generated by measuring the absorption of IR radiation by sample as a function of radiation frequencies, which is accomplished by an IR spectrometer. The absorption band of a specific bond is called the characteristic band of this bond (Thompson, 2018).

IR spectrometer has been commercially available since the 1940 s. Dispersive spectrometer is used at that time, constituted by light source, spectroscope, monochromator and detector. Prisms or gratings are used as monochromator to disperse radiations of varying wavelengths for the detection. An infrared spectrum is obtained by comparing the intensity of reference radiation and probing radiation. However, this instrument suffers from slow speed and low resolution. Nowadays, dispersive spectrometer is rarely used. The most important advance in IR instrument has come about as a result of the introduction of Fourier-transform (FT) technique. In the mid-1960 s, the first commercial FTIR spectrometer became available, and it was widely used after the mid-1970 s (Griffiths, 2017). FTIR spectrometer consists of light source, Michelson interferometer, detector and computer. Taking Michelson interferometer as its core, FTIR spectrometer is based on the interference of light. The measured interferogram is transformed to an infrared spectrum by a computer through Fourier transforms. FTIR spectrometer has several advantages over dispersive spectrometer, including Fellgett's advantage, Jacquinot's advantage and Connes advantage. The Fellgett's advantage is that radiation over a wide range can be measured simultaneously by a single detector in the FTIR spectrometer, which enables a faster analysis speed. Taking advantage of a J-stop aperture, FTIR spectrometer can provide a higher wavenumber resolution. This is so-called Jacquinot's advantage. Connes advantage means FTIR spectrometer can determine wavenumbers accurately, which provide high reliability and reproducibility. These advantages make FTIR spectrometer the most widely used type of IR spectroscopy (Tasumi, 2014).

There are numerous advantages of FTIR spectroscopy in molecular structure elucidation: 1) it is almost universal for many different types of samples; 2) it is a sensitive technique with minimum amount of sample required; 3) the acquisition process is relatively easy and fast; 4) the information in spectrum is abundant; 5) the cost is relatively low. However, this technique is not perfect. There are also some drawbacks of FTIR spectroscopy. For example, it has a higher requirement of testing environment. Atmosphere humidity and carbon dioxide can drastically affect the spectrum quality and hinder spectrum interpretation. FTIR spectroscopy also suffers from the limitation of analyzing mixtures, which is the biggest practical challenge FTIR spectroscopy faces (Smith, 2011). The difficulty of spectrum interpretation and band assignment increases with the complexity of the analyte composition.

Interpretation of polysaccharide IR spectrum

IR spectra of polysaccharides are generally complicated and difficult to interpret directly. FTIR spectrum provides well divided absorption region of characteristic groups, which can simplify the interpretation process and provide a useful guide for carbohydrates identification (Wiercigroch, et al., 2017). Though the chemical mechanism of these absorption is not discussed in details, it can be found elsewhere, for example, *Infrared Spectroscopy* (Thompson, 2018) and *Introduction to experimental infrared spectroscopy: Fundamentals and practical methods* (Tasumi, 2014). Normally, attentions should be paid to five spectral regions in polysaccharide IR spectrum listed as follows:

Region I: 4000–2500 cm^{-1}. Commonly, a strong and broad band at 3600–3000 cm^{-1} region can be found in the IR spectrum of polysaccharide. This intense band corresponds to the stretching vibration of abundant OH in polysaccharide. In addition, a well resolved group of moderate bands located at 3000–2500 cm^{-1} region can be assigned to the symmetric and asymmetric stretching vibrations of skeletal CH and CH_2 in polysaccharides (Wang, Xin, Yin, Huang, Wang, Hu, et al., 2022).

Region II: 1800–1500 cm^{-1}. This region is so-called "double bonds stretching" region. Bands in this region can be assigned to stretching vibrations of double bonds. The COO– doublet which is characteristic for pectic polysaccharides is located in this region (Wan, Hong, Shi, Yin, Koev, Nie, et al., 2021). In addition, a water band appears at about 1635 cm^{-1} in this region and can shift depending on the strength of interactions.

Region III: 1500–1200 cm^{-1}. This region is considered as "the local symmetry" region, mainly including deformational vibrations of groups with local symmetry, such as CH_2 and the numerous C-OH deformations encountered in carbohydrates (Wiercigroch, et al., 2017). However, due to the overlap of different bands of different vibrations, this region is relatively crowded and the assignment of observed bands by classical group-frequencies correlations is challenging.

Region Ⅳ: 1200–800 cm^{-1}. In general, the region of frequencies between 1200 cm^{-1} and 800 cm^{-1} may be called "fingerprint" region (Pasandide, Khodaiyan, Mousavi, & Hosseini, 2017). Compared with monosaccharides, the appearance of new bands in 1175–1140 cm^{-1} region is believed to be the result of glycosidic linkage formation in polysaccharide. Different configurations of glycosidic linkages lead to differences in the 1000–920 cm^{-1} region (Nikonenko, Buslov, Sushko, & Zhbankov, 2005). In addition, bands in the 900–800 cm^{-1} region, which is called anomeric region, can be used to differentiate the α and β configuration of anomeric carbon (Wang, et al., 2022).

Region Ⅴ: Blow 800 cm^{-1}. This region is known as the "skeletal region". As its name suggested, bands in this region are related to the carbohydrate skeletal vibrations (Wiercigroch, et al., 2017). However, information of polysaccharide structure given in this region is limited and rarely discussed.

Classical applications of IR spectroscopy

Qualitative characterization

Based on observations of characteristic absorptions, IR spectroscopy has been widely employed for qualitative characterization of polysaccharides. Main application areas include the identification of polysaccharide types, substitution groups, anomeric carbon configurations, and crystal allomorphs. However, due to the similarity of polysaccharide structure, the qualitative analysis of polysaccharides by IR spectroscopy is a challenging task. In addition, the overlap of bands in spectra may mask some characteristic information, which further increases the difficulty of this analysis. Thus, it may be empirical and unreliable to perform qualitative analysis of polysaccharides by only one characteristic IR peak. To improve the accuracy of this methodology, a group of characteristic bands are needed. Besides, some chemometric tools can be employed to extract useful information from complex spectra and improve reliability of qualitative analysis.

Identification of polysaccharide types

With the help of chemometric tools such as principal component analysis (PCA), IR spectroscopy has been applied to identify the type of

isolated polysaccharide and existence of specific polysaccharides in complex system such as PCW. The most informative spectral region used for this identification is 1800–800 cm^{-1}.

Polysaccharide components in PCW of a broad range of fruits and vegetables have been assessed by IR coupled with multivariate analyses. It was found that bands at 1075, 1440–1450, 1616 and 1740 cm^{-1} were characteristic for pectin and bands at 895, 1035–1041 and 1160–1163 cm^{-1} were characteristic for cellulose (Canteri, Renard, Le Bourvellec, & Bureau, 2019). In the research conducted by Liu, Renard, Bureau, & Le Bourvellec (2021), in which 58 cell wall polysaccharides from different sources was analyzed by IR spectroscopy and PCA, key wavenumbers for different polysaccharides were identified. Band at 988 cm^{-1} was assigned to cellulose and bands at 1740 and 1600 cm^{-1} were attributed to pectin. Band at 1035 cm^{-1} was characteristic for xylose-containing hemicelluloses, while bands at 1065 and 807 cm^{-1} were used for the identification of mannose-containing hemicelluloses. Similar results can be found in the IR analysis of PCW compositions in tomato and apple during development (Chylińska, Szymanska-Chargot, & Zdunek, 2016; Szymanska-Chargot, Chylinska, Kruk, & Zdunek, 2015).

Other polysaccharides can also be identified by IR spectroscopy. Several polysaccharide food additives, including starch, β-glucan, galactan, glucomannan, pectin and carrageenan, were characterized by PCA analysis of FTIR spectra. Results indicated that glucose and galactose-based polysaccharide could be distinguished in PC1 by negative band at 998 cm^{-1} and positive band at 1068 cm^{-1}, respectively. Pectin was discriminated in PC2, by bands at 1145, 1100, 1018, and 960 cm^{-1} in the negative side and 1064 and 1045 cm^{-1} in the positive side. And ι- and κ-carrageenans were separated from other polysaccharides by bands at 929 and 848 cm^{-1} (Černá et al., 2003). In addition, Boulet, Williams, & Doco (2007) collected IR spectra of 15 polysaccharides previously purified from red wine and performed overall analysis of these spectra using PCA. Four major families of polysaccharides were found, including mannoproteins, arabinogalactan-proteins, RG-I and RG-II. Significant differences were found among different polysaccharide families.

Identification of substitution groups

There are many different types of substitution groups in polysaccharide chains, naturally existed or chemically installed. Their existences are reported to have relation with bioactivities of polysaccharides (Luo, Zhang, Wu, & Zhao, 2021). IR spectroscopy is a reliable analytical method used to confirm existences of different substitution groups in polysaccharides, due to its sensitivity, quick readout, and minimal sample requirement (Caputo et al., 2019). It can also be applied to follow the progress of substitution reaction of synthetic substituted polysaccharides, as the attachment of substitution groups to polysaccharide backbone results in new absorption bands in the IR spectra (Korva, Karkkainen, Lappalainen, & Lajunen, 2016). Some common substituent groups in polysaccharides including sulfonyl, acetyl, phosphoryl and carboxymethyl groups and their characteristic wavenumbers are summarized in Table S1.

Sulphated polysaccharides are a group of diverse polymers including natural heparin, carrageenan, fucoidan and some chemically synthetic sulphated polysaccharides (Arlov et al., 2021). Three characteristic absorption bands at 1200–1270 cm^{-1}, 1010–1060 cm^{-1} and 900–800 cm^{-1}, corresponding to symmetric, asymmetric stretching of S═O and stretching of C—O—S, respectively, can be used to confirm the attachment of sulfonyl groups to polysaccharides (Caputo et al., 2019). Additionally, by comparing IR spectra of carrageenans with sulphate substituent at different position, Korva et al. (2016) found that the location of sulphate substituents can be discriminated by wavenumber of C—O—S vibration at 900–800 cm^{-1}.

Acetyl groups are present in polysaccharides in two forms, *O*-linked and *N*-linked, respectively. *O*-linked acetyl groups are commonly found in plant-derived polysaccharides and synthetic polysaccharides while *N*-linked acetyl groups are usually found in chitin and chitosan. Both of them can be characterized by stretching vibration of C═O and symmetric bending vibration of CH_3. The latter is identical for both, with a strong absorption at 1365–1380 cm^{-1}. However, stretching vibration of *O*-linked C═O has an absorption at around 1740 cm^{-1}, while that of *N*-linked C═O has an absorption at about 1640 cm^{-1}. In addition, *O*-linked and *N*-linked acetyl groups can be distinguished by the absorption of C—O vibration and C—N vibration at around 1245 cm^{-1} and 1550 cm^{-1}, respectively (Lucas et al., 2021; Shi et al., 2017).

Phosphorylated polysaccharides have been widely found in nature, meanwhile several chemically modified methods have been applied to synthesize phosphorylated polysaccharides by replacing hydroxyl groups of polysaccharides with phosphate groups (Chen & Huang, 2018). Existence of phosphoryl groups in polysaccharide can be identified by the vibration of P═O stretching and C—O—P bending, corresponding to absorptions at around 1250 and 915 cm^{-1}, respectively (Wang et al., 2018).

Methylated polysaccharide is the intermediate products of methylation analysis, which is a classic method for primary structure characterization of polysaccharide. Fully methylation of hydroxyl groups in polysaccharides is essential for this analysis. Complete methylation of polysaccharide can be confirmed using FTIR spectroscopy by monitoring the disappearance of the band at OH stretching region (3000–3500 cm^{-1}) of the spectrum. Meanwhile, the intensity of stretching vibration of alkyl groups (–CH_2- and –CH_3) at about 2930 cm^{-1} will significantly increase (Liu et al., 2019).

Carboxymethylated polysaccharides and selenylated polysaccharides are important chemically modified polysaccharide derivatives. The emergence of two new strong absorptions at 1600 and 1420 cm^{-1} can be used to confirm the successfully carboxymethylated modification of polysaccharide. In addition, bands at about 1250 cm^{-1} and 1070 cm^{-1}, corresponding to asymmetrical and symmetrical stretching of C—O—C, are also important for this confirmation (Theis et al., 2019). Diagnostic peaks for selenylation modification are at 1080 cm^{-1}, 850 cm^{-1} and 610 cm^{-1}, which can be attributed to stretching of O-Se-O, Se = O and Se—O—C, respectively (Fiorito et al., 2018).

Identification of anomeric carbon configurations

One monosaccharide adopts four different configurations in solution, two different anomeric carbon configurations (α or β) and two types of sugar ring (furan and pyran). However, once glycosidic bond is formed, the configuration of anomeric carbon is fixed (Guo, Ai, & Cui, 2018). Configuration differences could result in totally different physicochemical properties. For example, amylose and cellulose, with 1,4-α-D-glucopyranose and 1,4-β-D-glucopyranose as building block respectively, have totally different water-solubility. Hence, configuration identification is an important subject of polysaccharide structure elucidation. Configurations of anomeric carbon can be distinguished by both IR and NMR, but considering the time and cost required, IR may be a better choice.

As mentioned above, specific bands in anomeric region are useful for the identification of anomeric carbon configurations. As shown in Table 1, three absorption peaks at 1000–1200 cm^{-1} range indicate the existence of pyranose forms while there are only two absorptions in this area of furanose forms. Band at about 890 cm^{-1} indicates the existence of β-configuration while bands at 840 cm^{-1} or 920 cm^{-1} indicate the existence of α-configuration. Multiple bands at region 920–840 cm^{-1} indicate the presence of both α and β configuration. However, some inconsistency can be found in different reports, which may be due to different sources, different sampling methods and different IR instruments.

Identification of crystal allomorphs

The existence of abundant intra- and inter-molecular hydrogen bonds and different organizations of cellulose chains lead to various crystalline structures (Reiniati, Hrymak, & Margaritis, 2017). Hitherto, six crystalline polymorphs of cellulose including cellulose I, II, III_I, III_{II},

Table 1
Characteristic wavenumbers of anomeric carbon configurations.

α-configuration	β-configuration	Pyran ring	Furan ring	References
836.2 cm^{-1}	902.1 cm^{-1}	768.9 cm^{-1}	800.3 cm^{-1} and 923.8 cm^{-1}	(Molaei & Jahanbin, 2018)
	882.00 cm^{-1}	1050.07 cm^{-1}		(Xu et al., 2016)
835.2 cm^{-1}		774.6 cm^{-1}		(Sahragard & Jahanbin, 2017)
840 cm^{-1} or 920 cm^{-1}	890 cm^{-1}	three absorption peaks in 1000–1200 cm^{-1} range		(Zhang et al., 2018)
860.14 cm^{-1}		1155.21 cm^{-1}, 1080.72 cm^{-1} and 1022.14 cm^{-1}		(Zhi et al., 2019)
864.6 cm^{-1}			996.1 cm^{-1} and 1070.6 cm^{-1}	(Zou, Du, Hu, & Wang, 2019)
829 cm^{-1}		1024 cm^{-1} and 1085 cm^{-1}		(Jiang et al., 2020)
		1000 cm^{-1} and 1200 cm^{-1}		(Hajji et al., 2019)
847.3 cm^{-1}	891.6 cm^{-1}	1024.5 cm^{-1}, 1080.9 cm^{-1} and 1154.2 cm^{-1}		(Li et al., 2017)
	901.71 cm^{-1}	1043.15 cm^{-1}, 1073.47 cm^{-1} and 1160.69 cm^{-1}		(Wang et al., 2017)
	892 cm^{-1}	1046 cm^{-1}		(Yan et al., 2018)

IV_I, and IV_{II} have been reported. Naturally occurring cellulose is identified as cellulose I and it can be converted into other polymorphs by different treatments. Additionally, cellulose I is comprised of two slightly different allomorphs, I_α and I_β, which are formed by triclinic and monoclinic cell unit, respectively (Rongpipi, Ye, Gomez, & Gomez, 2019). Differences of hydrogen bond networks in cellulose crystalline polymorphs can be reflected by their absorptions of OH stretching in IR spectra. Thus, by monitoring these absorptions, IR spectroscopy can be used for the discrimination of different polymorphs (Makarem et al., 2019). For example, cellulose I_α was characterized by absorptions at 3240 and 750 cm^{-1} and cellulose I_β was identified by bands at 3270 and 710 cm^{-1} (Sugiyama, Persson, & Chanzy, 1991). Spectra features at region 3700–2700 cm^{-1} of cellulose I_β, II, III_I and III_{II} were compared in Fig. 1A. It was found that cellulose I_β was featured by band at 3320 cm^{-1}. Cellulose II was characterized by bands at 3480 cm^{-1}, 3440 cm^{-1} and a shoulder peak at 3150 cm^{-1}. Only one band at 3480 cm^{-1} was found in the spectrum of cellulose III_I and no characteristic band was assigned for cellulose III_{II} due to its low crystallinity (Lee et al., 2013).

According to their distinguished X-ray diffraction (XRD) patterns, crystalline polymorphs of starch can be classified into three types (A, B or C type) (Han, Shi, & Sun, 2020). A-type starch is formed by monoclinic unit cell, which is more compact with lower water content. B-type starch is formed by hexagonal unit cell with a hydrated helical core which is more open with water molecules. C-type starch is believed to be the mixture of A- and B-type starch (Wang, Xu, & Luan, 2020; Wu, Witt, & Gilbert, 2013). It is controversial that whether IR spectroscopy can be used to distinguish these crystalline polymorphs. Sevenou, Hill, Farhat, & Mitchell (2002) compared IR spectra of wheat starch (A-type) and potato starch (B-type) and found that their spectra features were identical. Thus, they concluded that FTIR spectroscopy was not suitable for starch crystalline polymorphs discrimination and the correlations between IR and XRD described in pervious papers may be misleading. Similar conclusion was draw by Warren, Gidley, & Flanagan (2016), after comparing IR spectra features of a wider range of samples including 61 starches in dry and hydrated states. They believed that longer range associations in starches which was related to crystalline structure could not be distinguished by FTIR spectroscopy because it could only reflect short range molecular interactions. However, Pozo et al. (2018) held a divergent opinion. They believed that above researches were suffered from attenuated total internal reflectance (ATR) acquisition mode of IR spectra. With this mode, structure information reflected in IR spectra only refered to the surface of the sample. Thus, FTIR spectroscopy with transmission mode was applied to discriminate crystalline types of 13 starches. By analyzing IR spectra with PCA, they found that B-type starch was well distinguished from A- and C-type starches.

Quantitative characterization

According to the Beer-Lambert principle, the absorption intensity of analyte is related to its concentration. Theoretically, quantification of specific compounds can be calculated by the intensity of its characteristic bands if there is no interference from other materials. However, it is recognized that IR spectrum is always crowded with overlapped bands. Therefore, the critical step for quantitative analysis of a specific component is to find out its characteristic bands and eliminate interferences from other compounds. Manipulations of spectral data are needed to achieve it.

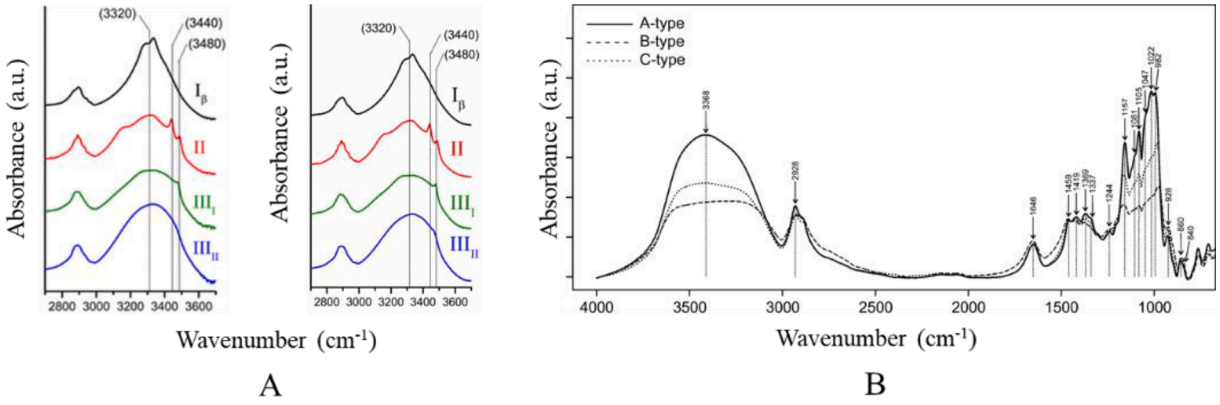

Fig. 1. IR spectra of cellulose and starch crystalline polymorphs. A. Cellulose I_β, II, and III_I, and III_{II} from Avicel cellulose (left) and α-cellulose (right), reprinted with permission from Springer Nature (Lee et al., 2013). B. Type-A, B, and C starches, reprinted with permission from Springer Nature (Pozo et al., 2018).

Determination of polysaccharide content

Generally, polysaccharide content can be determined by time-consuming wet chemistry based analytical methods. The combination of IR and chemometric tool provides an alternative solution without handling-intensive pretreatment for this determination. This rapid and regnant-free method is particularly suitable for high throughput analysis and quality control of commercial polysaccharides.

A typical application of this method is the determination of polysaccharide composition in PCW. Pectin, cellulose and hemicellulose contents in PCW material of 16 different fruits were predicted by FTIR spectroscopy and partial least squares regression (PLS) analysis (Chylińska, Szymańska-Chargot, Kruk, & Zdunek, 2016). Coupling with PLS analysis, ATR-FTIR spectroscopy was employed to determine polysaccharide composition in 29 plant species. These indicated that this method could serve as a generic quatitative tool for PCW polysaccharide from a large diversity of plants (Canteri et al., 2019). Additionally, this method was also performed to the determine the composition changes of polysaccharides in apple cell wall during different development stages (Szymanska-Chargot et al., 2015).

FTIR can also be used to determine the content of other polysaccharides such as fructan, fucoidan and mannan. The feasibility of applying ATR-IR spectroscopy and PLS analysis to determine fructan content in barley, malt and onion was validated (Clark, Shaw, Wright, & McCallum, 2018; Cozzolino, Roumeliotis, & Eglinton, 2014). The purity of fucoidan from brown seaweed was also determined by this method. Estimated fucoidan content using IR-based method were close to that using the HPLC-RI (High performance liquid chromatography-refractive index) method, which indicated the high prediction accuracy of this method (Zhao, Garcia-Vaquero, Przyborska, Sivagnanam, & Tiwari, 2021). It could also be applied to identify and predict content of fucoidan and fructan in their mixture, which was useful for adulteration preventing (Espinosa-Velazquez, Ramos-de-la-Pena, Montanez, & Contreras-Esquivel, 2018). FTIR spectroscopy coupling with PLS analysis could also be applied to determine carbohydrate composition of *Saccharomyces cerevisiae*, including trehalose, mannan and glycogen (Plata, Koch, Wechselberger, Herwig, & Lendl, 2013).

Determination of substitution degree

Substitution degree of polysaccharide is an important factor that affects its physicochemical properties and functional features. Several methods have been developed to determine this parameter, such as NMR, gas chromatography and potentiometric titration. Compared with these methodologies, FTIR spectroscopy provides appreciable advantages for this determination, benefitting from its simplicity, speediness and practicability.

Degree of methylesterification (DM) is one of the important factors of pectin that affects its functional properties, defined as percentage of galacturonic acid esterified by methanol in pectin. In general, two distinct bands in the 1800–1600 cm^{-1} region respectively corresponding to esterified and free carboxyl groups can be applied to determine the DM of pectin. This determination was based on the area ratio of bands for ester carboxyl and total carboxyl (Monsoor, Kalapathy, & Proctor, 2001). Other than isolated pectin, this method was also proved to be reliable to evaluate DM of pectin in extracted cell wall from papaya fruit (Manrique & Lajolo, 2002). The presence of water or other carboxyl groups containing components such as proteins in complex system may interfere with the accuracy of this method. Thus, some treatments of obtained spectra such as curve-fitting (Chatjigakis et al., 1998) and spectra deconvolution (Kyomugasho, Christiaens, Shpigelman, Van Loey, & Hendrickx, 2015) is necessary to eliminate such interferences. Except based on bands at the 1800–1600 cm^{-1} region, Fellah, Anjukandi, Waterland, & Williams (2009) proposed that DM of pectin could be determined based on bands at 1440 cm^{-1} for asymmetric stretching of CH_3 and 1010 cm^{-1} for backbone vibration. This alternative approach could also eliminate interferences from other compounds.

Degree of *O*-acetylation substitution of cellulose can be determined by FTIR based method, by calculating the height ratio or area ratio of band representing acetyl groups to band representing cellulose. Selection of these bands is crucial due to the possible band overlap of cellulose and acetyl groups. Stefke, Windeisen, Schwanninger, & Hinterstoisser (2008) selected bands at 1745 or 1240 cm^{-1} to represent acetyl groups and band at 1030 cm^{-1} to represent cellulose. However, Li, Cai, & Zhang (2019) thought the selection of cellulose representing band was doubtful because the absorption of symmetrical stretching of acetate at 1030 cm^{-1} would overlap with this band. Instead, band at 1164 cm^{-1} related to antisymmetrical bridge oxygen stretching in cellulose skeleton was chosen to represent cellulose in their methodology.

Degree of *N*-acetylation (DA) substitution is an important term to distinguish chitin and chitosan. Chitin is mainly composed of *N*-acetyl-glucosamine, while chitosan is the deacetylation product of chitin (Crini, 2019). In general, when DA is below 40%, chitosan is formed. Similarly, DA of them can be calculated by ratio of bands corresponding to amide group in *N*-acetyl-glucosamine to bands representing group existed in both glucosamine and *N*-acetyl-glucosamine. Different bands selected for this determination were well reviewed by Kasaai (2008). However, this methodology was believed to suffer from inaccuracies especially for chitosans with low DA. Recently, a new approach based on FTIR and partial least squares (PLS) was proposed. A good PLS model was obtained by taking spectral region from 1800 to 1500 cm^{-1} as dataset. This model was robust and highly precise even for chitosans with low DA (Dimzon & Knepper, 2015).

FTIR coupled with PLS regression has also been applied to evaluate the degree of substitution (DS) of carboxymethyl starch (CMS). An optimal PLS regression model with 6 PLS factors was obtained with a coefficient of determination (R^2) of 0.9593 and root-mean-square error of cross validation (RMSECV) of 0.0141. Then, the prediction set gave a R^2 of 0.9368 and standard deviation ratio (SDR) of 2.09, respectively, which indicated that this model was suitable for DS prediction of CMS (Liu, Chen, Dong, Ming, & Zhao, 2012).

Determination of crystallinity index

According to the classic two-phase model, cellulose was believed to contain two regions, crystalline and amorphous regions. Parameter crystallinity index (CI) is commonly utilized to quantify the ratio of crystalline regions in cellulose materials. Different techniques including NMR, XRD, Raman spectroscopy and IR spectroscopy have been used for the determination of cellulose CI. IR spectroscopy-based methodology for CI determination is realized by measuring relative areas or intensities of various characteristic peak related to crystallinity.

Three classical terms used to describe CI of cellulose are lateral order index (LOI), total crystallinity index (TCI), and hydrogen bond intensity (HBI) (Kruer-Zerhusen, Cantero-Tubilla, & Wilson, 2018; Tribulová, Kacik, Evtuguin, Cabalova, & Durkovic, 2019). Different characteristic IR bands are used for the calculation of this index. LOI, also called empirical CI, is expressed as ratio of band intensities at 1427 cm^{-1} to 895 cm^{-1}, proposed by Hurtubise and Krassig (1960). Band at 1427 cm^{-1}, known as crystalline band, can be ascribed to the symmetric scissoring vibration of CH_2 at C6. Band at 895 cm^{-1}, known as amorphous band, corresponding to C—O stretching vibration of cellulose ring. Relative amounts of crystalline regions versus amorphous parts in cellulose is reflected by this ratio (Rongpipi et al., 2019). TCI, proposed by Nelson and Oconnor (1964), is calculated as the ratio of band intensities at 1375 cm^{-1} to 2900 cm^{-1}. Absorption at 1375 cm^{-1} corresponds to C—H bending of amorphous cellulose. Absorption at 2900 cm^{-1} can be attributed to CH_2 and C—H stretching which are independent of crystallinity. HBI, proposed by Nada, Kamel, & El-Sakhawy (2000), is determined by ratio of band intensities at 3336 cm^{-1} to 1335 cm^{-1}. Band at 3336 cm^{-1} is assigned to O—H stretching vibrations while band at 1335 cm^{-1} represents C—H rocking of cellulose ring.

These three classical parameters were widely used in cellulose crystallinity determination by IR spectroscopy, together or alone. Based on this methodology, CI change of cellulose in silver fir wood before and

after metal ions treatments was studied (Tribulova et al., 2019). Correlation between cellulase activity and cellulose crystallinity was investigated by determining CI values of cellulose digestion products (Kruer-Zerhusen et al., 2018). CI change of cellulose from tobacco stems during pulp beating process was also explored (Zhao et al., 2017). In these studies, good correlations were found between results from IR spectroscopy-based methodology and those from XRD or NMR.

A three-band ratio algorithm (R_2) based on bands at 800–700 cm^{-1} region has also been developed to assess the crystalline information of cotton fibers. This algorithm was expressed as follows, $R_2 = (I_{708}\text{-}I_{800})/(I_{730}\text{-}I_{800})$. Absorption at 800 cm^{-1} was selected as background reference for normalization. Bands at 708 cm^{-1} and 730 cm^{-1} represented crystalline cellulose I_β and amorphous cellulose, respectively. CI_{IR} can be converted from R_2 by Eq. $CI = (R_2\text{-}R_{2,sm})/(R_{2,lr}\text{-}R_{2,sm})$, in which R_2 means the R_2 values for unknown sample, $R_{2,lr}$ and $R_{2,sm}$ represent the largest R_2 and the smallest R_2 values, respectively (Kim, Liu, French, Lee, & Kim, 2018; Liu, Thibodeaux, Gamble, Bauer, & VanDerveer, 2012).

A method based on FTIR spectroscopy was proposed for the determination of relative crystalline (RC) of starch. A probe band (varying with crystallinity) and a reference band (acting as internal standard to eliminate errors) were selected for this calculation. Through the investigation of starch spectra, band between 1300 and 800 cm^{-1} region was defined as a probe band. As shown in Fig. S1, a Gaussian fitting peak at this region was used as a reference band. Finally, a hypothesis was proposed that there was a Gaussian holocrystalline-peak (HCP) in the spectrum of starch at the 1300–800 cm^{-1} region and it could be divided into two parts. One part overlapped with experimental FTIR spectrum of starch was believed to be crystalline region, and the remaining part was assigned as amorphous region. RC of starch was measured as the area ratio of crystalline region to HCP. This hypothesis was validated by comparing RC values of different starches obtained from this method with those from XRD. The good agreement between two approaches demonstrated that this independent FTIR spectroscopy-based method was suitable for RC determination of starch (Sun et al., 2014).

Advanced IR techniques and their applications

It is a trend to broaden the application of IR by integrating with other techniques. Some advanced IR techniques and their advantages are introduced in Table 2. The combination of IR with MS makes it possible to record the mass information and IR fingerprint of mass selected ion simultaneously. FTIR microspectroscopy can image and visualize PCW *in situ*, by not only identifying polysaccharides in PCW, but also determining their spatial distribution and relative abundance. With the help of theoretical computation like density functional theory (DFT), it is much easier to interpret the spectroscopic data with overlapping frequencies. This provides us with a promising tool to unravel structure of polysaccharides and PCW.

Integrating with MS

MS technique occupies an important position at the forefront of carbohydrate structure analysis owing to its speed and sensitivity. However, the inherent nature of MS determines that it is blind to ubiquitous isomerism of carbohydrates. IR spectroscopy is highly sensitive to even the slightest structural and conformational differences. Thus, the integration of MS and IR spectroscopy combines advantages of both sides and can simultaneously record mass information and IR fingerprint of selected carbohydrate fragments, which make it a promising way to overcome such blindness. There are two technical routes to realize the integration of MS and IR spectroscopy, room-temperature IR multiphoton dissociation (IRMPD)-MS and cryogenic IR spectroscopy-MS, as shown in Fig. 2.

Table 2
Advanced IR techniques and their application

Advanced IR techniques	Advantages	Applications
IR-MS	Providing MS and IR information simultaneously	Oligosaccharides or fragments from polysaccharides
IR-Microscopy	Providing spital distribution information of polysaccharide	Polysaccharides in plant cell wall
IR-DFT	Enabling the accurate assignment of bands in IR spectrum	Individual polysaccharide or polysaccharide in plant cell wall

IRMPD-MS and its applications

Rather than the measurement of direct absorption of IR radiation by analytes in classical IR spectroscopy, the change of analyte ions after absorption of IR photons is determined in IRMPD-MS experiments (Gray, Compagnon, & Flitsch, 2020). Classically, analyte ions are trapped inside an ion trap in the IRMPD-MS system. Then, an IR laser beam is injected inside the ion trap. Analyte ions can absorb multiple IR photons when its vibrational mode is resonant with the IR radiation. This absorption increases internal energy of target ion and thus leads to photofragmentation. Dissociation yield of trapped ion is measured by MS detector and then plotted as a function of wavenumber to develop an IR spectrum.

As summarized in Table 3, IRMPD-MS has been employed to differentiate isobaric phosphated and sulfated D-glucosamine (Schindler et al., 2014), positional isomers of sulfated monosaccharides (Schindler et al., 2017a), hexuronic acid epimers (Schindler et al., 2017c), ring-size of monosaccharides (Schindler et al., 2019), and anomers and conformers of monosaccharides (Barnes, Schindler, Chambert, Allouche, & Compagnon, 2017; Barnes, Allouche, Chambert, Schindler, & Compagnon, 2020). Larger carbohydrate molecules can also be distinguished by IRMPD-MS. Isomeric glycosaminoglycan (GAG) disaccharides with different sulfate patterns from chondroitin sulfate and heparin were well discriminated by their IRMPD spectroscopic signatures (Schindler et al., 2017a). Linkage isomers of sialic acid-containing trisaccharide in *N*-glycan and milk oligosaccharides displayed distinguished IRMPD fingerprints (Depland, Renois-Predelus, Schindler, & Compagnon, 2018). Four mono-*N*-deacetylated and two doubly-*N*-deacetylated chitosan tetramer with different patterns of *N*-acetylation were investigated by IRMPD-MS. Their unique MS and IR signatures demonstrated that the acetylation patterns of chitooligosaccharides could be well resolved without reducing end labelling (Wattjes et al., 2017). However, it is worth noting that the resolution of obtained spectra may decrease as the increase of carbohydrate size. Other than direct characterization of precursor ions, IRMPD-MS can also be performed on smaller collision induced dissociation generated product ions, which make it suitable for carbohydrate sequencing. By comparing the IR fingerprints of monosaccharide fragments from disaccharide precursor with monosaccharide standards, Schindler et al. (2017b) found that monosaccharide content of precursor could be retrieved by IR analysis of its fragmentation product and the stereochemistry memory of glycosidic bond was kept by anomeric configuration of product ion. Based on these findings, they proposed the basic principles of a generic method for oligosaccharide sequencing and validate it by a crude chitooligosaccharide sample. This strategy has also been successfully applied to elucidate epimeric forms of hexuronic acid in hyaluronic acid tetrasaccharide (Schindler et al., 2017c). Now that structural information of precursor ion is transposable to fragmentation product ion, resolution of IR spectra can be improved by IRMPD analysis of fragmentation product. This was validated by IRMPD analysis of positional isomers of sulfated disaccharides and tetrasaccharide and their fragmentation ions (Renois-Predelus, Schindler, & Compagnon, 2018).

Some upstream separation techniques prior to IRMPD characterization were developed to enable the prefractionation of carbohydrate mixture. With the help of a so-called “stop flow” mood during IRMPD acquisition time in HPLC method, Schindler et al. (2018) established the

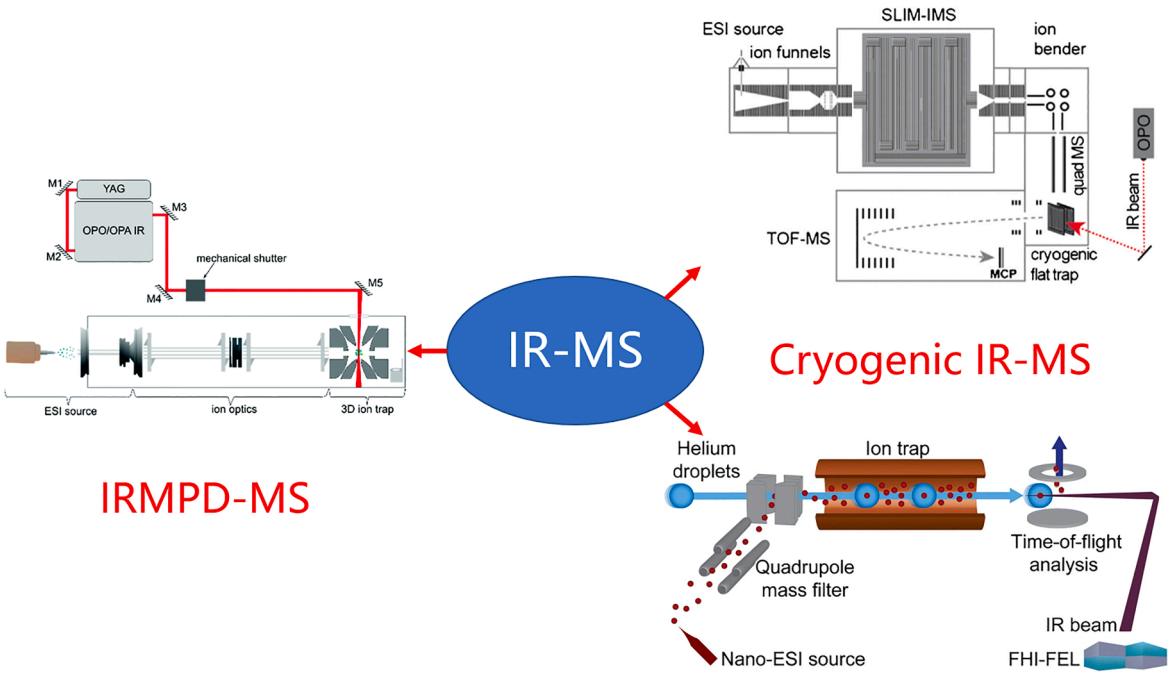

Fig. 2. Schematic overview of IR-MS instruments in different technical routes, reprinted with the permission from American Chemical Society (Warnke, Ben Faleh, Scutelnic, & Rizzo, 2019); from Springer Nature (Lettow et al., 2019); from Royal Society of Chemistry (Schindler et al., 2019).

first online novel LC-MS-IRMPD workflow. As shown in Fig. 3, this approach performed well in distinguishing disaccharides regioisomers and monosaccharide anomers, which showed great promises for carbohydrate sequencing. In addition, a capillary isotachophoresis method for GAGs separation was proposed for off-line coupling with IRMPD spectroscopy. It was suitable for sample at microseparation scale and the purity of separated fraction was high enough for IRMPD analysis (Jaravel et al., 2020).

Cryogenic IR-MS and its applications

As discussed above, IRMPD-MS has been widely used and may provide abundant details about carbohydrate structure. However, some spectra display poor resolution with broad bands and many highly characteristic features may be masked. Conformational flexibility of carbohydrate ions at room temperature and thermal activation of ions upon sequential absorption of IR photons may lead to this poor resolution (Gray et al., 2019). Cryogenic IR spectroscopy, which can provide higher resolution spectra by decreasing the number of ions at vibrational state in cryogenic environment, is applied to overcome this limitation (Khanal, Masellis, Kamrath, Clemmer, & Rizzo, 2018).

Cryogenic IR approach is generally performed with the help of so-called "messenger" molecules or atoms which are optical transparent, such as H_2, N_2 or He. Ions can be tagged with "messenger" via weak ion-induced dipole interactions during cooling process by the cold buffer gas. Dissociation between target ion and "messenger" induced by IR radiation resonant is monitored by MS and then plotted as a function of wavelength to generate IR spectrum of cryogenic ions.

In general, a drift-tube ion mobility spectrometry (IMS) is integrated to selectively separate carbohydrate ions according to their drift time before cryogenic IR analysis. Measured drift time can be converted into rotationally averaged collision cross-section (CCS), an instrument-independent data, which is only related to the size and shape of analyte (Hofmann, Hahm, Seeberger, & Pagel, 2015). Based on a home-built instrument that combines IMS with cryogenic IR spectroscopy and MS, Khanal, Masellis, Kamrath, Clemmer, & Rizzo (2017) identified five isomeric GAG disaccharides. Compared with relatively broad IRMPD spectra of their counterparts obtained by Schindler (2017a), spectral bands in this experiment were sharp and more distinctive for each isomers. With the improvement of spectral resolution, cryogenic IR-MS can be employed to directly identify larger carbohydrate molecules which may be hardly distinguishable in IRMPD-MS. For example, two mannose-based pentasaccharides, linear and branched mannopentaose, were successfully distinguished (Masellis, Khanal, Kamrath, Clemmer, & Rizzo, 2017). Similarly, a set of isomeric human milk oligosaccharides (HMOs), ranging from trisaccharides to hexasaccharides, were identified by their diagnostic cryogenic IR fingerprint (Khanal et al., 2018).

Recently, advance in IMS technology led to the emerge of so-called structures for lossless ion manipulations (SLIM)-based IMS. In a proof-of-principle experiment conducted by Ben Faleh, Warnke, & Rizzo (2019), the SLIM-IMS integrated with cryogenic IR-MS displayed ultrahigh resolution and was powerful enough to identify the composition of isomers mixtures, compared with drift-tube IMS. With this ultrahigh resolution, characteristic fingerprints for a series of larger carbohydrates, ranging from heptasaccharide to decasaccharide, were provided (Yalovenko, Yatsyna, Bansal, AbiKhodr, & Rizzo, 2020). The generality of anomeric retention during CID of carbohydrates was also investigated by cryogenic IR-MS conducted by Pellegrinelli et al. (2020). They validated the finding of Schindler et al. (2017b) and extended it from disaccharides to hexasaccharides, demonstrating that anomeric memory can be retained irrespective of fragment size and branching. Ulteriorly, the SLIM-IMS device was modified to incorporate a CID section in which fragmentation of precursor ion happened. This technique enabled the mobility separation of a parent ion and its fragments generated by CID. By analyzing these fragment ions by cryogenic IR-MS, a spectroscopic database of fragments was constructed and it could be used to identify parent carbohydrate structure. This approach was proved to have the ability to address fundamental questions regarding the glycosidic linkage fragmentation mechanism and showed the potential to identify structure of carbohydrates without commercially standards (Bansal et al., 2020). Dyukova, Carrascosa, Pellegrinelli, & Rizzo (2020) compared the cryogenic IR spectra of carbohydrates after enzymatic cleavages and their corresponding standards. They found that the cleaved products were highly structured and their cryogenic IR spectra were identical to their standard counterparts, which demonstrated that this combined strategy could be applied to identify unknown carbohydrates and construct a database of complex carbohydrates.

Table 3
Applications of IR-MS integration techniques in carbohydrate structural analysis.

Technical routes		Applications	Analytes	IR sources /wavenumber range	References
IRMPD-MS		Differentiation of D-glucosamine 6-phosphate vs. D-glucosamine 6-sulfate	Monosaccharide	OPO/ OPA* 3200–3700 cm^{-1}	(Schindler et al., 2014)
		Acetylation pattern diagnostic of chitooligosaccharides	Tetrasaccharide	OPO/ OPA 2800–3700 cm^{-1}	(Wattjes et al., 2017)
		Sulfate pattern diagnostic of GAG	Disaccharide	OPO/ OPA 2700–3700 cm^{-1} FEL 550–1850 cm^{-1}	(Schindler et al., 2017a)
		Hexuronic acid epimers identification in GAG	Tetrasaccharide	OPO/ OPA 2700–3700 cm^{-1}	(Schindler et al., 2017b)
		Anomeric memory of C-fragments during CID	Pentasaccharide	OPO/ OPA 2700–3700 cm^{-1}	(Schindler et al., 2017c)
		Conformational preferences of protonated *N*-acetylated hexosamines/ DFT simulation	Monosaccharide	OPO/ OPA 2700–3700 cm^{-1}	(Barnes et al., 2017)
		Development of LC-MS-IRMPD approach	Disaccharide	OPO/ OPA 2700–3700 cm^{-1}	(Schindler et al., 2018)
		Sulfate pattern analysis of CID product ion of GAG	Tetrasaccharide	OPO/ OPA 2700–3700 cm^{-1}	(Renois-Predelus et al., 2018)
		Linkage isomers identification of sialic acid-containing HMOs	Trisaccharide	OPO/ OPA 2700–3700 cm^{-1}	(Depland et al., 2018)
		Spectroscopic diagnostic for the ring-size of carbohydrates	Monosaccharide	OPO/ OPA 2700–3700 cm^{-1}	(Schindler et al., 2019)
		Analysis of anomers and conformers of glucosamine mixture/ DFT simulation	Monosaccharide	OPO/ OPA 2700–3700 cm^{-1}	(Barnes et al., 2020)
		Off-line coupling of capillary isotachophoresis separation to IRMPD-MS for isomeric GAG mixture analysis	Disaccharide	OPO/ OPA 2700–3700 cm^{-1}	(Jaravel et al., 2020)
Cryogenic IR-MS	Messenger-tagging	Carbohydrate isomers identification	Pentasaccharide	OPO/ OPA 3200–3700 cm^{-1}	(Masellis et al., 2017)
		Isomeric GAG identification	Disaccharide	OPO/ OPA 3200–3700 cm^{-1}	(Khanal et al., 2017)
		Isomeric HMOs identification	Hexasaccharide	OPO/ OPA 3200–3700 cm^{-1}	(Khanal et al., 2018)
		Development of SLIM-IMS integrating cryogenic IR spectroscopy and composition identification of HMOs isomers mixtures	Tetrasaccharide	OPO/ OPA 3200–3700 cm^{-1}	(Ben Faleh et al., 2019)
		Generality of anomeric retention C-fragments during CID	Hexasaccharide	OPO/ OPA 3200–3700 cm^{-1}	(Pellegrinelli et al., 2020)
		Identification of *N*-linked glycans cleaved from protein by comparing with standards	Decasaccharide	OPO/ OPA 3200–3700 cm^{-1}	(Yalovenko et al., 2020)
		Comparison of cryogenic IR spectra of selective enzymatic cleaved carbohydrates with standards	Nanosaccharide	OPO/ OPA 3200–3700 cm^{-1}	(Dyukova et al., 2020)
		Development of SLIM-CID-IMS integrating cryogenic IR spectroscopy	Hexasaccharide	OPO/ OPA 3200–3700 cm^{-1}	(Bansal et al., 2020)
	Superfluid Helium	Identification of a series of isomeric milk sugar	Tetrasaccharide	FHI FEL# 1000–1800 cm^{-1}	(Mucha et al., 2017)
		Observation of fucose migration in MS experiments	Tetrasaccharide	FHI FEL 1000–1800 cm^{-1}	(Mucha et al., 2018)
		Mechanism of fucose migration in intact ion	Tetrasaccharide	FHI FEL 1000–1800 cm^{-1}	(Lettow et al., 2019)
		Comparison of resolution of IRMPD-MS and cryogenic IR-MS	Pentasaccharide	FHI FEL 1000–1800 cm^{-1}	(Lettow et al., 2020)
		Anomeric retention of B-fragments during CID	Monosaccharide	FHI FEL 1000–1800 cm^{-1}	(Greis et al., 2020)

* OPO/ OPA means oscillator power amplifier-optical parametric oscillator laser
# FHI FEL means Fritz Haber Institute IR free-electron laser

An alternative cryogenic IR strategy without "messenger" molecules was developed by Mucha et al (2017). In this methodology, mass-to-charge (m/z) selected target ion was held inside an ion trap. Superfluid helium droplets with an average size of 10^5 helium atoms were guided through the trap to pick up ions and cooled them down to 0.37 K. Then, a tunable IR beam was injected to induce resonance with analyte ions. Unlike induced ion dissociation in IRMPD, this resonance led to ejection of ions from helium droplet. Ejection efficiency was monitored by time-of-flight (TOF) analysis and then was used to generate IR spectrum.

The carbohydrate differentiation potential of this methodology has been proved by a proof-of-principle experiment in which a series of structural well-defined carbohydrates, range from monosaccharide to tetrasaccharide, were well distinguished according to their highly diagnostic IR absorption patterns (Mucha et al., 2017). The complex GAG structure had also been investigated by this methodology and room-temperature IMPRD-MS. Obtained spectra of synthetic tetrasaccharides and pentasaccharides in the range from 1800 to 1000 cm^{-1} by two different methodologies were compared. It was not difficult to find that diagnostic bands in the IMPRD spectra were largely unresolved while resolved diagnostic features for monosaccharide composition and sulfation pattern were yielded in cryogenic IR spectra, which showed the higher resolution of this methodology (Lettow et al., 2020). Anomeric configuration memory retaintion in MS analysis, which was crucial for carbohydrate synthesis and sequencing, had also been investigated by this technique. While the generality that C-fragment can retain the anomeric memory of precursor ion had been proved as described above, the anomeric memory retation ability of B-type fragment ions was investigated by analysing a series of B-type fragments from protected galactoside precursors. Identical IR signatures of these fragments from different precursors, indicated that these B-type fragments can not retain anomeric memory like C-fragments do as metioned above (Greis et al.,

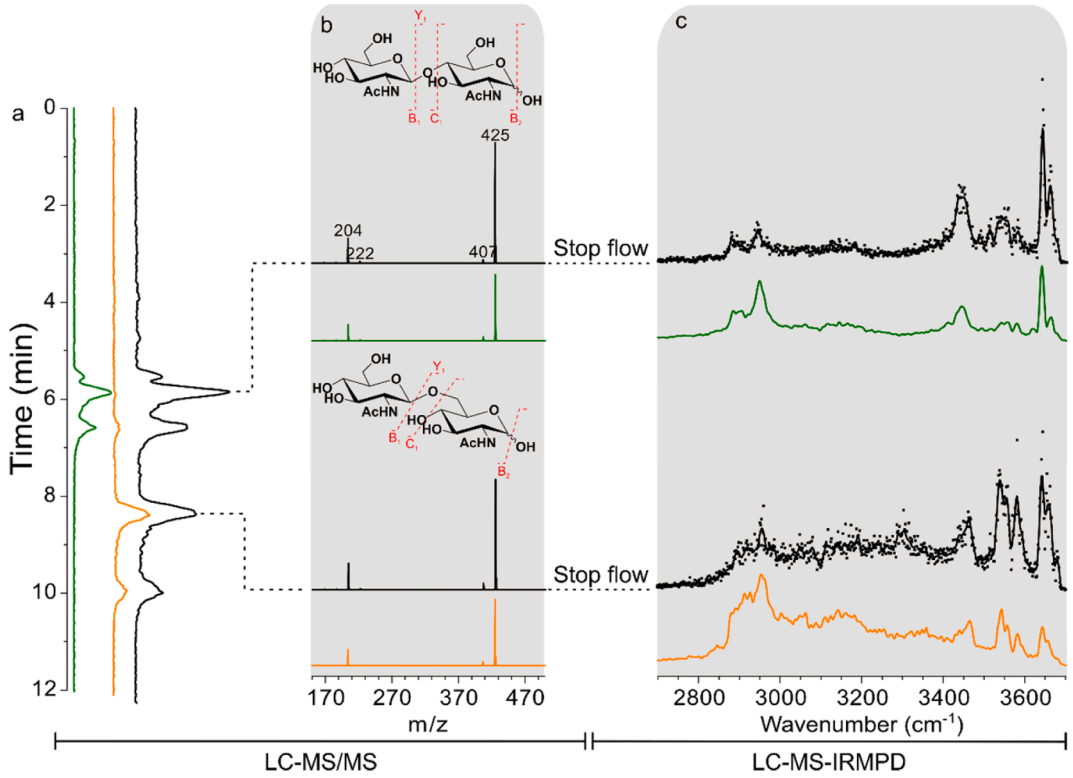

Fig. 3. Comparison of the performance of the LC-MS/MS and LC-MS-IRMPD workflows, reprinted with permission from American Chemical Society (Schindler et al., 2018).

2020).

Fucose migration, the intramolecular transfer of terminal fucose units to adjacent or remote monosaccharides upon activation, is a recurring observed problem in MS analysis process of fucose-containing carbohydrates, typically during CID. This migration may lead to misleading fragment ions generation and thus result in erroneous structural assignments in carbohydrate analysis. Above-mentioned methodology was utilized to investigate this migration phenomenon by comparing cold-ion IR spectra of three fucose-containing isomeric carbohydrates, the CID fragment of a tetrasaccharide Le^y and two intact trisaccharide standards Le^x and BG-H2. However, a surprising finding was observed that IR signatures for three structural isomers were almost identical. Since this technique has been proved to be highly diagnostic for even subtle structural variations, a possible explanation for this unforeseen finding is that these three isomeric carbohydrates, either CID product or intact precursor ion, undergo a fucose migration rearrangement reaction to the same structure, thus leading to identical IR spectra. This result implied that this migration is not only limited to CID ions and may be prevalent in any kind of MS experiment (Mucha et al., 2018). Based on above finding, the mechanism of fucose migration in intact ion was preliminary explored by cold-ion IR spectroscopy. It was found that a mobile proton at a specific site of the molecule was a prerequisite for fucose migration and the mobility of this proton can be affected by the presence of functional groups or adduct ions with competitive proton affinity (Lettow et al., 2019).

Concluding remarks

To date, the application scope of IR-MS is confined to relatively shorter carbohydrates such as monosaccharides and oligosaccharides. The larger size the analyzed ion is, the more congestive spectra will be. IRMPD-MS is suitable for monosaccharides and disaccharides differentiation. There are some reports that IRMPD spectral differences of isomeric pentasaccharides can be observed, but bands in spectra are broad and may sometimes overlap with each other that result in diagnostic details loss. The development of cryogenic IR-MS with higher resolution significantly improves spectra quality and makes the analysis of larger carbohydrate (up to decasaccharide) to be possible. Though it is still unknown if larger carbohydrates or even polysaccharide can be analyzed by this advanced technique directly, the outlook is bright thanks to continuous technological progresses and research efforts.

Now that the generality of anomeric retention during CID has been proved by both IRMPD-MS and cryogenic IR-MS, analysis of CID products ion rather than intact precursor ion will be an alternative strategy to improve spectra quality by decreasing analyte size. Selective enzymatic cleavage of larger carbohydrate is also another effective methodology, as identical IR spectra are found between cleaved products and reference standards. These two strategies are of benefit to carbohydrate spectroscopic database establishment, which will be an important complement of existing carbohydrate database. What has to be aware of is that carbohydrates currently analyzed by IR-MS are mainly mammalian derived, such as GAGs and HMOs. More carbohydrates, especially plant-derived polysaccharide, should be involved to enrich this carbohydrate spectroscopic database.

IR-MS analysis of CID products and selective enzymatic cleavage products have also been validated to be capable for carbohydrates sequencing. Meanwhile, efforts have also been made to reduce the spectrum acquisition time from minute level to second level, which make this technique suitable for high-throughput analysis. In addition, development of several upstream separation techniques coupling with IR-MS make the analysis of carbohydrates in a complex mixture system possible. All of these developments illustrate that IR-MS can sever as an important tool for glycomics.

Developments in IR light source have enabled more detailed structural information observed in IR-MS experiments. Normally, an IR laser beam is employed in IR-MS system. It is generated by a YAG-pumped OPO/OPA system tunable in the 3 μm region, where OH groups typically absorb photons strongly. Recent advance in free-electron laser (FEL) enables the scan of a wider spectra range and provides spectra

with unprecedented resolution in fingerprint region. However, this instrument is only accessible to a few groups and far from commercial applications. Thus, research and development of user-friendly and commercially available instruments are important to get more groups involved in this filed and crucial to more extensive applications of this advanced technology.

To summarize, combination of IR with MS is a relatively new but powerful technique compared with established carbohydrate structural analysis method. While applications of this technique in precise structural differentiation of carbohydrates increase rapidly and many progresses have been achieved during recent years, it is quite clear that some further developments are needed.

FTIR microspectroscopic imaging

PCW, the main origin of plant-derived polysaccharides, is a complex system including polysaccharide components (e.g., cellulose, hemicellulose and pectin) and non-carbohydrate substrates (e.g., lignin, protein and lipid). FTIR microspectroscopic imaging is a label-free imaging technique which can not only identify polysaccharides in PCW but also determine their spatial distribution and relative abundance (Türker-Kaya & Huck, 2017; Zhao, Man, Wen, Guo, & Lin, 2019). Based on the non-destructive character, it is capable of studying polysaccharides in PCW *in situ* during different periods or in different environments (Wu et al., 2019).

Since the 1990 s, FTIR microspectroscopic technique has been wildly employed in PCW analysis. Benefited from technical advances of both hardware and software aspects in recent years, acquisition time has been reduced drastically and image quality has been largely improved (Cheng & Xie, 2015). In the hardware part, IR synchrotron radiation with high brightness is applied to reach higher signal intensities with high spatial resolution; the advanced ATR acquisition mode has shown great potential in water containing samples; establishment of focal plane array (FPA) imaging systems by an array of miniature detector elements allows simultaneous recordation of thousands of spectra over an area (Gierlinger, 2018; Wellner, 2013). In the software part, by dint of multivariate unmixing methods and chemometric methods, the assignment and interpretation of spectra with many overlapping bands can be successfully completed as well as chemical distributions and semi-quantitative chemical information of polysaccharide in PCW can be provided (Bhargava, 2012).

Applications in crop stalks

FTIR microspectroscopic imaging was used to provide insight into crop stalks by so-called "IR dissection" of its transverse section. A typical monocotyledonous crop and a typical dicotyledonous crop, corn and cotton, were taken as examples. IR bands at 1240 cm^{-1}, 1040 $cm^{-1}$and 1504 cm^{-1} were used as diagnostic spectral peaks for cellulose, hemicelluloses and lignin, respectively. Spatial distribution and relative concentration of polysaccharides were intuitively displayed by chemical images at characteristic wavelengths. Principal components analysis (PCA) was applied to compare differences between different tissues of crop stalks by spectra data (Cao, Yang, Han, Jiang, & Ji, 2015). But it is difficult to find a diagnostic wavelength for image generation if components with similar spectra coexist. A more elaborate chemometric method, fast non-negativity-constrained least squares (fast NNLS)

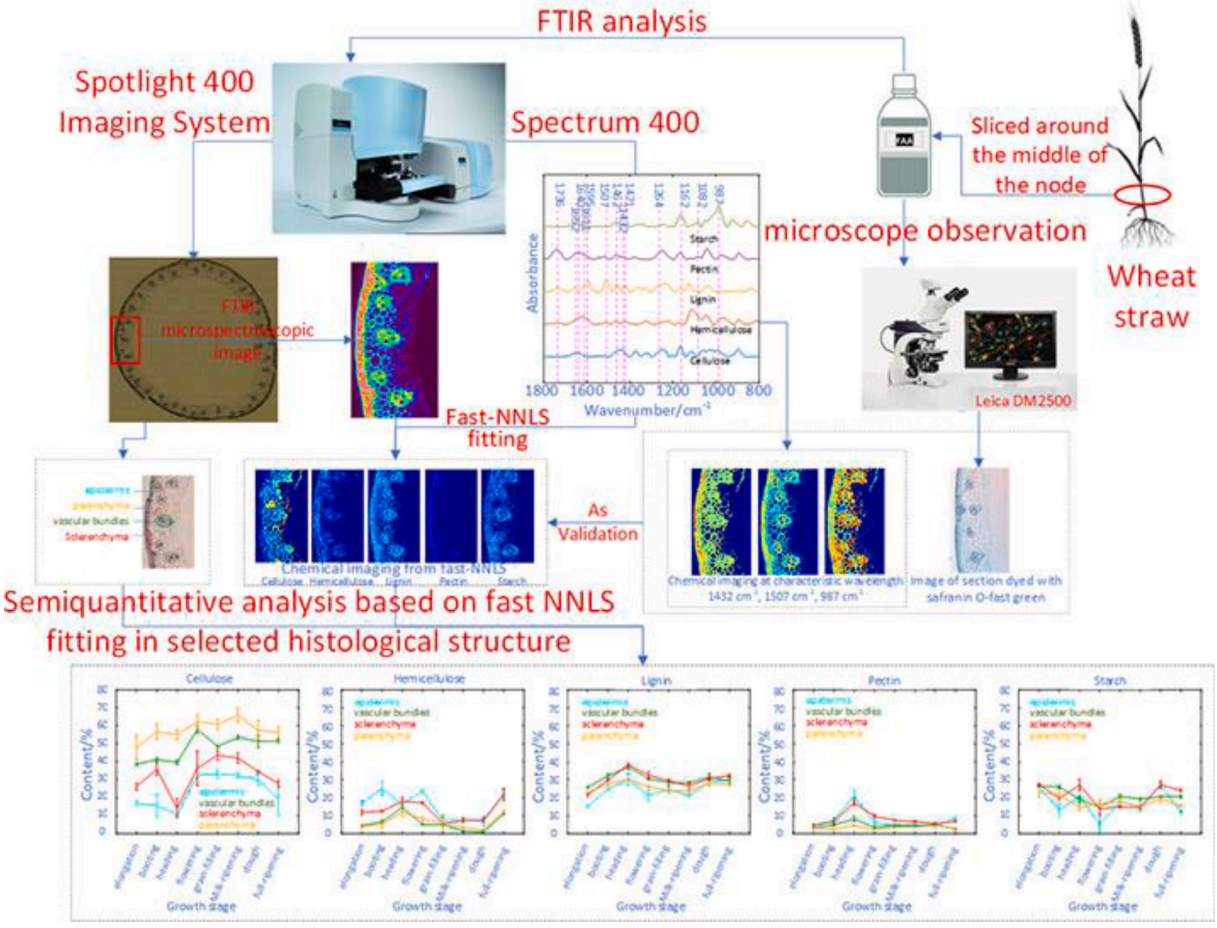

Fig. 4. Visualization and semiquantitative of major components in wheat straw by FTIR microspectroscopic imaging and fast NNLS fitting, reprinted with permission from American Chemical Society (Yang et al., 2018).

algorithm, can be applied to handle such problem. As shown in Fig. 4, FTIR microspectroscopic imaging and the fast NNLS algorithm were employed to characterize a wheat straw transverse section *in situ*. This method is capable to provide spital distribution and semiquantitative information of cellulose, starch, hemicellulose and pectin. Imaging results based on fast NNLS algorithm were consistent with results from tissue-dyeing and chemical imaging at characteristic wavelengths. In addition, changes of chemical composition in various tissues during different growth stages were observed by semiquantitative analysis of main components via fast NNLS fitting (Yang et al., 2018). A novel FTIR imaging scheme based on multivariate calibration analysis coupled with calibration transfer was developed by Li, Wei, Xu, Xu, & He (2018) to achieve quantitative visualization of cellulose and hemicellulose in bamboo transverse sections at microscopic view. Compared with chemical imaging based on single characteristic wavelength, this scheme was capable to avoid the interferences of bands overlap between absorptions of different compounds and provide quantitative visualization information rather than semiquantitative analysis.

Applications in fruits

Changes of polysaccharides distribution and composition in PCW are closely associated to fruit softening during postharvest storage. FTIR microspectroscopic imaging is capable to visualize polysaccharides changes in spatial dimension during softening process in a label-free way, so as to provide a better understanding of fruit softening mechanism. Softening process of peaches stored at 0 °C and 20 °C was observed by FTIR microspectroscopic imaging. Bands at 1250–1230 cm^{-1}, 1050–1030 cm^{-1}, and 1760–1740 cm^{-1} were employed for the visualization of cellulose, hemicellulose and pectin, respectively. It was clear to observe that main polysaccharide components were dispersed throughout the peach cell wall and have intensive IR absorption in the cell corner from IR images. As storage time increased, polysaccharides in cell wall began to degrade gradually. The degradation rate of pectin was found to be slower than those of cellulose and hemicellulose. Lower storage temperature significantly delayed the degradation process and prolonged the storage life of peach (Huang et al., 2020). Besides the softening process of fruit from hard to soft, FTIR microspectroscopic imaging can also be utilized to investigate the maturation process of nut shell that from soft to hard. IR bands at 1036 cm^{-1}, 1734 cm^{-1} and 1504 cm^{-1} were used for the imaging of cellulose, hemicellulose and lignin distribution, separately. Components changes of different parts and different growth stages in walnut shell were presented by IR intensity-based color-coded maps. Differences of outer and inner parts between July and October samples confirmed by PCA analysis indicated that the secondary cell wall was thickened and the content of cell wall components were increased during maturation process of walnut shell (Xiao et al., 2020).

Applications in woods

FTIR microspectroscopic imaging can also provide insight to complex wood cell wall composition at the cellular level. Cuello and coworkers (2020) proposed a high-throughput microphenotyping workflow based on ATR-FTIR microspectroscopy and developed a multivariate IR image analyses method including automatic pixel clustering and identification of differentially absorbed wavenumbers (DAWNs) among samples, as shown in Fig. 5. This technique was applied to study three types of poplar wood grown in different environments, normal wood of staked trees (NW), tension and opposite wood of artificially tilted trees (TW, OW). Mechanical strains put on TW and OW induced changes in chemical composition of wood cell wall. Ten cell wall samples from different cell wall layers of different cell types in three kinds of trees were collected and investigated. The identification of polysaccharides such as crystalline cellulose, acetylated xylans, and hemicelluloses were achieved by correctly assigned DAWNs. This novel technique is a high-throughput tool that is useful for microphenotyping of cell walls and understanding the relationship between cell wall compositions and cell wall differences (Cuello et al., 2020).

Concluding remarks

FTIR microspectroscopic imaging technique is the combination of FTIR spectroscopy and microscopic imaging techniques. Conventional FTIR spectroscopy can only provide an average spectrum without any spital information. Microscopic imaging techniques enable the visualization of specific components. Their combination has been applied to provide new insights into polysaccharide information at cellular level in different types of PCW.

Though various progresses have been achieved, there are still several restrictions. One problem is the relatively low spatial resolution restricted by the diffraction limitation. Another one is the interpretation of spectra with overlapping bands from different polysaccharides. Further work should focus on both improvements of instruments to obtain better spatial resolution and optimizations of data processing

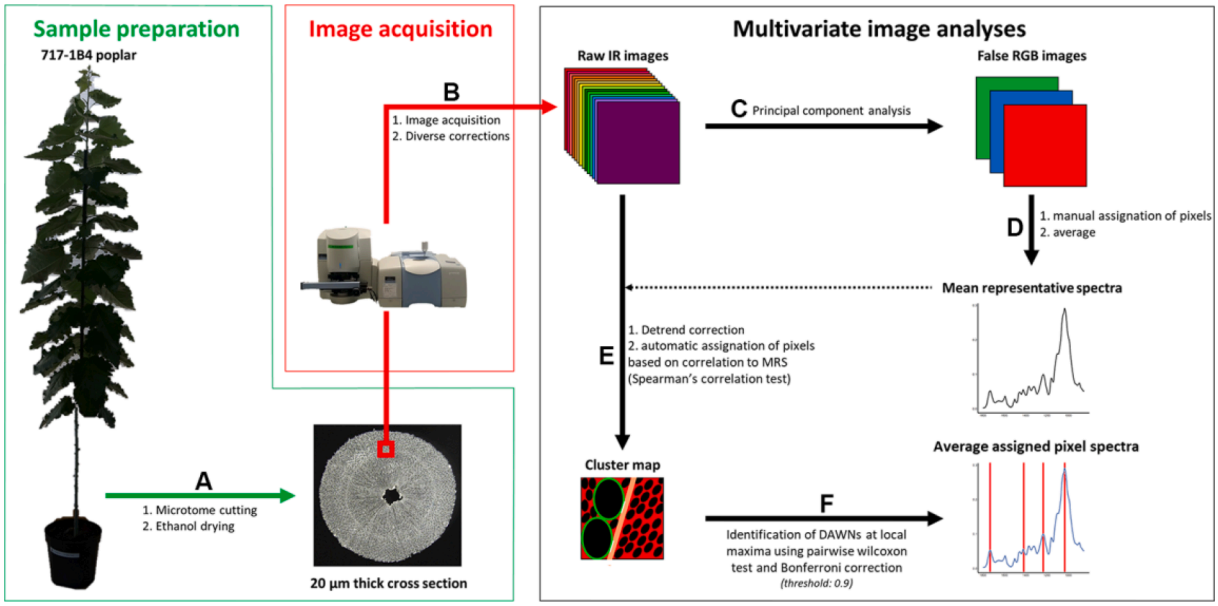

Fig. 5. High-throughput microphenotyping workflow of poplar cell wall, reprinted with permission from Frontiers Media SA (Cuello et al., 2020).

methods to acquire specific spectra for polysaccharides. Besides, the combination of other imaging techniques such as Raman micro-spectroscopy and atomic force microscopy will help to gain a better understanding of polysaccharide microstructures in PCW.

Integrating with density functional theory

IR spectroscopy can provide abundant details on polysaccharide structure but the interpretation of obtained spectra may be ambiguous and empirical sometimes. A critical step of IR spectra interpretation is the accurate assignment of absorption bands to corresponding functional groups. However, it is challenging when bands from different groups overlapped with each other. Density functional theory (DFT) is a computational quantum mechanical modelling method that investigates the electronic structure of multi-electronic system by electronic density. It can help the interpretation process of IR spectroscopic data, but its inherent uncertainty and error can lead to inaccuracies especially when the number of atoms included in the system of interest grows. Several calculation methods such as B3LYP, wB97X-D and mPW1PW91 are used for DFT calculation. After the model is optimized, harmonic frequency calculations is used to provide vibrational frequencies and IR intensities. Simulated IR spectra can be converted from above data by a Lorenzian line shape function. When IR spectroscopy and DFT can be used in a complementary way, the advantages of both can be maximized. Accuracy of DFT can be improved by benchmarking calculated results against IR data, in turn, an accurate DFT method can be applied to explain spectra of unknow samples. The combination of IR spectroscopy and DFT can serve as a promising tool toward unraveling structure of polysaccharides (Kubicki, Yang, & Kim, 2019).

Applications in individual polysaccharides

In a proof of principle experiment on cellulose vibrations prediction and assignation by DFT calculations performed by Barsberg (2010), simple single chain cellulose models were used for the first time to reproduce main features of cellulose I IR spectrum. Predicted results provided theoretical basis for cellulose IR bands assignation. It could also be used to identify the molecular origin of so-called cellulose "marker" bands, for example, 750 and 710 cm^{-1}, which were used to distinguish cellulose crystal in I_α and I_β forms, and the ratio of 1426 cm^{-1} and 896 cm^{-1} was defined as cellulose crystallinity index. It is worth noting that this approach is just a first-order approximation and further improvements are needed. Periodic DFT calculations coupled with dispersion corrections (DFT-D2) was used for cellulose structure modeling. Good correlation was found between observed vibrational frequencies and calculated IR frequencies of I_α and I_β cellulose, indicating that this methodology was reliable to reproduce experimental IR spectrum of cellulose and help interpret experimental data. Its calculated results were trustable even when performed on materials that were not well constrained experimentally such as ''amorphous'' or disordered cellulose (Kubicki, Mohamed, & Watts, 2013). Water is an important component in PCW and the interaction between water and cellulose in the interface is critical to the chemical reactivity of cellulose. Above approach was also performed on different I_α and I_β cellulose surfaces with and without hydrated H_2O molecules. Though observed spectra were not reproduced accurately, relative order of calculated and experimental frequencies were in good agreement. Meanwhile, the ability of DFT calculation to corelate each frequency with corresponding vibrational modes made the interpretation of broad spectra of cellulose-water interface much easier (Kubicki, Watts, Zhao, & Zhong, 2014). Different hydrogen bonding networks in cellulose crystals were modeled by DFT and power spectra obtained by Car-Parrinello molecular dynamics (CPMD) were compared with experimental IR spectra. Stretch vibrational modes of each OH in the power spectra were assigned by this comparison. Calculation results showed that hydrogen bonding network models I_β(A) and II(B) were more stable and the calculated power spectra of them were in better agreement with experimental IR spectra than those of models I_β(B) and II(A) (Hayakawa, Nishiyama, Mazeau, & Ueda, 2017).

As mentioned in section 3.2.2, Fellah et al. (2009) proposed a new methodology to determine the DM of pectin samples based on bands corresponding to C—H stretches rather than those related to carboxylate groups. Accuracy of this approach was confirmed from theoretical perspective by DFT calculations of monomeric-, dimeric-, and trimeric-pectic compounds with different DM. Compared with experimental spectra of pectin with different DM, main spectral features could be reproduced by DFT stimulation. This method has also been employed to investigate the covalent coupling of pectin and polystyrene beads. Stimulated spectra of galacturonic acid dimers, bead intermediates, and covalently coupled products were generated by DFT calculations and compared with experimental spectra. Combined with DFT calculation, IR spectroscopy could provide strong evidences for success coupling of pectin and bead substrate by monitoring the formation of a new C—N bond in IR spectrum. The consistency between experimental spectra and calculated spectra validated the reliability of this methodology (Fellah, Anjukandi, Hemar, Otter, & Williams, 2011). A pectin with a DM of 76% was isolated from citrus peel and then investigated by IR spectroscopy. Two galacturonic acid dimers, one with both COOH and COO-CH_3 groups (Ac) and the other one with two COO-CH_3 groups (Es), were considered to be two subunits that constitute this pectin. They were stimulated by Hybrid B3LYP/6-31G* method in gas and aqueous phases. Reasonable correlation was found between stimulated spectra and experimental spectra, as shown in Fig. 6. By using the normal internal coordinates and the scaled quantum mechanical procedure, 141 normal vibration modes for Es and 132 normal vibration modes for Ac were completely assigned. According to bands assignments of calculated and experimental spectra, several IR bands at 3436 (OH), 1743 (CO), 1640 (CO), 1146 (CO glycosidic), 1103 (CO) and 1017 (CO glycosidic) cm^{-1} were picked as characteristic peaks for pectin and could be applied for quick identification of pectin by IR spectroscopy (Bichara et al., 2016).

Detailed interpretation of IR spectra arabinogalactan (AG) and its sulphated derivatives (SAG) was performed with the help of DFT. Since AG was mainly composed of galactose, both AG and SAG were modeled based on two galactose units. Good correlations between calculated and experimental spectra were found for AG and SAG. Bigger difference between theoretical and experimental spectra was observed in SAG than AG, because the addition of sulphur groups could increase the possibility of isomers and conformers (Kazachenko et al., 2020).

Applications in complex polysaccharides system

The combination of IR spectroscopy and DFT has shown potential to investigate polysaccharide structure in more complex system such as PCW. It was applied to interpret the vibrational changes of palm kernel cake (PKC) before and after enzymatically hydrolyzation and fermentation. Main polysaccharide components, cellulose and mannan, were modeled and many characteristic bands of them were assigned by comparing experimental and theoretical spectra. Assignment results were applied to interpret IR spectra of PKC before and after treatments. Obvious degradation and removal of mannan were reflected by the intensity decline of characteristic bands in the 950–800 cm^{-1} region. In addition, an interesting phenomenon of band position shift was observed. Band corresponding to CH_2 wagging of cellulose shift from 893 cm^{-1} to 889 cm^{-1} of PKC after treatment, indicating that the environmental change of cellulose C6-OH group due to degradation of closely linked cellulose or mannan chains. The positional shift of mannan at 1180 cm^{-1} might be related to the DP decrease of mannan (Barsberg, Sanadi, & Jorgensen, 2011). DFT method at the RB3LYP/6-31G (d,p) level was applied to model a series of algae polysaccharide based on their dimeric units. By comparing spectral features of experimental spectra of crude polysaccharides extracted from 11 algae, standard spectra of commercial algae polysaccharide standards and their theoretical spectra, major polysaccharide components in different algae were identified (Fernando et al., 2017). Berezin et al. (2017) stimulated

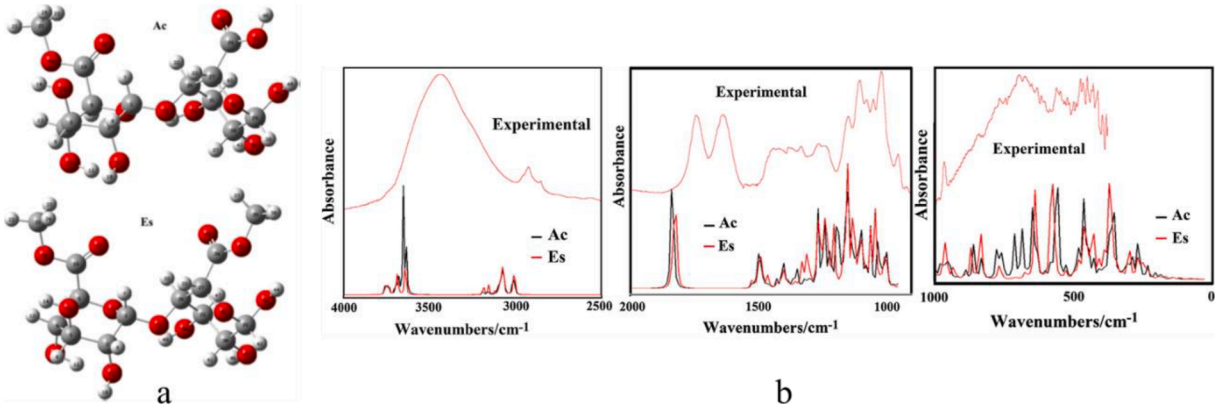

Fig. 6. Theoretical molecular structure and comparison between experimental and theoretical IR spectra. a. theoretical molecular structure of Ac and Es. b. comparison between the experimental IR spectra of pectin with theoretical spectra of Ac and Es, reprinted with permission from Elsevier (Bichara et al., 2016).

IR spectra of individual components such as cellulose, hemicellulose, pectin, in lemon peel cell wall based on DFT method at the RB3LYP/6-31G(d) level. Then, a model of PCW consisting of these compounds was constructed and a group spectrum of this model was stimulated theoretically. Compared with the experimental spectrum of lemon peel, a good agreement was observed. Detailed interpretation of experimental spectrum was performed with the help of theoretical model and the contribution of each individual component to different bands was assigned.

Concluding remarks

The accurate assignment of bands in IR spectrum to specific groups is a big challenge, while DFT calculation can help us to overcome it. The complementary nature of the IR spectroscopy and DFT enhances their respective advantages and makes up for each other's weaknesses. As mentioned above, good agreements are found between theoretical spectra and experimental spectra of polysaccharides. However, there are still some problems for the coupling. Considering that polysaccharides are macromolecules with high molecular weight, DFT simulation is mainly restricted by computational constraints and the size of the simulation model is limited. Thus, the accuracy of DFT should be improved by employing higher quality DFT functionals and basis sets.

Summary and outlook

Polysaccharide structure is the basis for understanding bioactivities of polysaccharide. Several techniques have been used for the polysaccharide structure analysis. There is no doubt that IR spectroscopy is one of the most widely applied tools. The low cost, high efficiency and high accessibility make it a well-accepted technique for routine analysis, and quality control of polysaccharide. This review has introduced the conventional applications of IR spectroscopy in polysaccharide structural analysis from the perspective of qualitative and quantitative characterization. However, it has played a subsidiary but not indispensable role in polysaccharide structure elucidation for a long time. The complexity of IR spectra and difficulty of precise spectra interpretation limit the applications. Notwithstanding these limitations, it is obvious that IR spectroscopy will play an important role in characterization procedure of polysaccharide. Further developments call for better spectrum quality and more precise band assignments to improve the accuracy of IR spectroscopy in polysaccharide structure analysis.

In addition, the emergence of IR integrating techniques have considerably expanded the application range of IR spectroscopy. IR-MS integrating techniques can provide multi-dimensional structural information and enable precise structural differentiation of carbohydrates. IR imaging sheds a light on the microstructure of polysaccharides in PCW by providing their spatial distribution and relative abundance information *in situ*. Combination of IR spectroscopy and DFT enables precise interpretation of IR spectra of polysaccharides, and may be applied to discriminate unknown sample.

Declaration of Competing Interest

The authors declare that they have no known competing financial interests or personal relationships that could have appeared to influence the work reported in this paper.

Acknowledgements

The financial supports from the National Key R&D Program of China (2018YFE0108300), and National Science Fund for Distinguished Young Scholars of China (31825020) were gratefully acknowledged.

Appendix A. Supplementary data

Supplementary data to this article can be found online at https://doi.org/10.1016/j.fochx.2021.100168.

References

Arlov, Ø., Rütsche, D., Asadi Korayem, M., Öztürk, E., & Zenobi-Wong, M. (2021). Engineered Sulfated Polysaccharides for Biomedical Applications. *Advanced Functional Materials, 31*(19), 2010732. https://doi.org/10.1002/adfm.v31.1910.1002/adfm.202010732

Bansal, P., Yatsyna, V., AbiKhodr, A. H., Warnke, S., Ben Faleh, A., Yalovenko, N., … Rizzo, T. R. (2020). Using SLIM-Based IMS-IMS Together with Cryogenic Infrared Spectroscopy for Glycan Analysis. *Analytical Chemistry, 92*(13), 9079–9085.

Barbosa, J. R., & de Carvalho Junior, R. N. (2021). Polysaccharides obtained from natural edible sources and their role in modulating the immune system: Biologically active potential that can be exploited against COVID-19. *Trends in Food Science & Technology, 108*, 223–235.

Barnes, L., Allouche, A.-R., Chambert, S., Schindler, B., & Compagnon, I. (2020). Ion spectroscopy of heterogeneous mixtures: IRMPD and DFT analysis of anomers and conformers of monosaccharides. *International Journal of Mass Spectrometry, 447*, 116235. https://doi.org/10.1016/j.ijms.2019.116235

Barnes, L., Schindler, B., Chambert, S., Allouche, A.-R., & Compagnon, I. (2017). Conformational preferences of protonated N-acetylated hexosamines probed by InfraRed Multiple Photon Dissociation (IRMPD) spectroscopy and ab initio calculations. *International Journal of Mass Spectrometry, 421*, 116–123.

Barsberg, S. (2010). Prediction of Vibrational Spectra of Polysaccharides-Simulated IR Spectrum of Cellulose Based on Density Functional Theory (DFT). *Journal of Physical Chemistry B, 114*(36), 11703–11708.

Barsberg, S., Sanadi, A. R., & Jørgensen, H. (2011). A new Density Functional Theory (DFT) based method for supporting the assignment of vibrational signatures of mannan and cellulose-Analysis of palm kernel cake hydrolysis by ATR-FT-IR spectroscopy as a case study. *Carbohydrate Polymers, 85*(2), 457–464.

Ben Faleh, A., Warnke, S., & Rizzo, T. R. (2019). Combining Ultrahigh-Resolution Ion-Mobility Spectrometry with Cryogenic Infrared Spectroscopy for the Analysis of Glycan Mixtures. *Analytical Chemistry, 91*(7), 4876–4882.

Berezin, K. V., Shagautdinova, I. T., Chernavina, M. L., Novoselova, A. V., Dvoretskii, K. N., & Likhter, A. M. (2017). The experimental vibrational infrared

spectrum of lemon peel and simulation of spectral properties of the plant cell wall. *Optics and Spectroscopy, 123*(3), 495–500.
Bhargava, R. (2012). Infrared Spectroscopic Imaging: The Next Generation. *Applied Spectroscopy, 66*(10), 1091–1120.
Bichara, L. C., Alvarez, P. E., Fiori Bimbi, M. V., Vaca, H., Gervasi, C., & Brandán, S. A. (2016). Structural and spectroscopic study of a pectin isolated from citrus peel by using FTIR and FT-Raman spectra and DFT calculations. *Infrared Physics & Technology, 76*, 315–327.
Boulet, J. C., Williams, P., & Doco, T. (2007). A Fourier transform infrared spectroscopy study of wine polysaccharides. *Carbohydrate Polymers, 69*(1), 79–85.
Canteri, M. H. G., Renard, C. M. G. C., Le Bourvellec, C., & Bureau, S. (2019). ATR-FTIR spectroscopy to determine cell wall composition: Application on a large diversity of fruits and vegetables. *Carbohydrate Polymers, 212*, 186–196.
Cao, C., Yang, Z., Han, L., Jiang, X., & Ji, G. (2015). Study on in situ analysis of cellulose, hemicelluloses and lignin distribution linked to tissue structure of crop stalk internodal transverse section based on FTIR microspectroscopic imaging. *Cellulose, 22*(1), 139–149.
Caputo, H. E., Straub, J. E., & Grinstaff, M. W. (2019). Design, synthesis, and biomedical applications of synthetic sulphated polysaccharides. *Chemical Society Reviews, 48*(8), 2338–2365.
Černá, M., Barros, A. S., Nunes, A., Rocha, Sílvia. M., Delgadillo, I., Čopíková, J., & Coimbra, M. A. (2003). Use of FT-IR spectroscopy as a tool for the analysis of polysaccharide food additives. *Carbohydrate Polymers, 51*(4), 383–389.
Chatjigakis, A. K., Pappas, C., Proxenia, N., Kalantzi, O., Rodis, P., & Polissiou, M. (1998). FT-IR spectroscopic determination of the degree of esterification of cell wall pectins from stored peaches and correlation to textural changes. *Carbohydrate Polymers, 37*(4), 395–408.
Chen, L., & Huang, G. (2018). The antiviral activity of polysaccharides and their derivatives. *International Journal of Biological Macromolecules, 115*, 77–82.
J.-X. Cheng X.S. Xie Vibrational spectroscopic imaging of living systems: An emerging platform for biology and medicine Science 350 6264 2015 aaa8870 aaa8870.
Chylińska, M., Szymańska-Chargot, M., Kruk, B., & Zdunek, A. (2016). Study on dietary fibre by Fourier transform-infrared spectroscopy and chemometric methods. *Food Chemistry, 196*, 114–122.
Chylińska, M., Szymańska-Chargot, M., & Zdunek, A. (2016). FT-IR and FT-Raman characterization of non-cellulosic polysaccharides fractions isolated from plant cell wall. *Carbohydrate Polymers, 154*, 48–54.
Clark, C. J., Shaw, M. L., Wright, K. M., & McCallum, J. A. (2018). Quantification of free sugars, fructan, pungency and sweetness indices in onion populations by FT-MIR spectroscopy. *Journal of the Science of Food and Agriculture, 98*(14), 5525–5533.
Cozzolino, D., Roumeliotis, S., & Eglinton, J. (2014). Feasibility study on the use of attenuated total reflectance MIR spectroscopy to measure the fructan content in barley. *Analytical Methods, 6*(19), 7710–7715.
Crini, G. (2019). Historical review on chitin and chitosan biopolymers. *Environmental Chemistry Letters, 17*(4), 1623–1643.
Cuello, C., Marchand, P., Laurans, F., Grand-Perret, C., Lainé-Prade, V., Pilate, G., & Déjardin, A. (2020). ATR-FTIR Microspectroscopy Brings a Novel Insight Into the Study of Cell Wall Chemistry at the Cellular Level. *Frontiers in Plant Science, 11*. https://doi.org/10.3389/fpls.2020.0010510.3389/fpls.2020.00105.s00110.3389/fpls.2020.00105.s00210.3389/fpls.2020.00105.s00310.3389/fpls.2020.00105.s004
Cui, F., Zhao, S., Guan, X., McClements, D. J., Liu, X., Liu, F., & Ngai, T.o. (2021). Polysaccharide-based Pickering emulsions: Formation, stabilization and applications. *Food Hydrocolloids, 119*, 106812. https://doi.org/10.1016/j.foodhyd.2021.106812
Depland, A. D., Renois-Predelus, G., Schindler, B., & Compagnon, I. (2018). Identification of sialic acid linkage isomers in glycans using coupled InfraRed Multiple Photon Dissociation (IRMPD) spectroscopy and mass spectrometry. *International Journal of Mass Spectrometry, 434*, 65–69.
Dimzon, I. K. D., & Knepper, T. P. (2015). Degree of deacetylation of chitosan by infrared spectroscopy and partial least squares. *International Journal of Biological Macromolecules, 72*, 939–945.
Dyukova, I., Carrascosa, E., Pellegrinelli, R. P., & Rizzo, T. R. (2020). Combining Cryogenic Infrared Spectroscopy with Selective Enzymatic Cleavage for Determining Glycan Primary Structure. *Analytical Chemistry, 92*(2), 1658–1662.
Espinosa-Velazquez, G., Ramos-de-la-Pena, A. M., Montanez, J., & Contreras-Esquivel, J. C. (2018). Rapid physicochemical characterization of innovative fucoidan/fructan powders by ATR-FTIR. *Food Science and Biotechnology, 27*(2), 411–415.
Fellah, A., Anjukandi, P., Hemar, Y., Otter, D., & Williams, M. A. K. (2011). Towards polysaccharide handles for single molecule experiments: Spectroscopic evidence for the selective covalent coupling of terminal sugar residues to desired substrates. *Carbohydrate Polymers, 86*(1), 105–111.
Fellah, A., Anjukandi, P., Waterland, M. R., & Williams, M. A. K. (2009). Determining the degree of methylesterification of pectin by ATR/FT-IR: Methodology optimisation and comparison with theoretical calculations. *Carbohydrate Polymers, 78*(4), 847–853.
Fernando, I. P. S., Sanjeewa, K. K. A., Samarakoon, K. W., Lee, W. W., Kim, H.-S., Kim, E.-A., … Jeon, Y.-J. (2017). FTIR characterization and antioxidant activity of water soluble crude polysaccharides of Sri Lankan marine algae. *Algae, 32*(1), 75–86.
Fiorito, S., Epifano, F., Preziuso, F., Taddeo, V. A., & Genovese, S. (2018). Selenylated plant polysaccharides: A survey of their chemical and pharmacological properties. *Phytochemistry, 153*, 1–10.
Gierlinger, N. (2018). New insights into plant cell walls by vibrational microspectroscopy. *Applied Spectroscopy Reviews, 53*(7), 517–551.
Gray, C. J., Compagnon, I., & Flitsch, S. L. (2020). Mass spectrometry hybridized with gas-phase InfraRed spectroscopy for glycan sequencing. *Current Opinion in Structural Biology, 62*, 121–131.
Gray, C. J., Migas, L. G., Barran, P. E., Pagel, K., Seeberger, P. H., Eyers, C. E., … Flitsch, S. L. (2019). Advancing Solutions to the Carbohydrate Sequencing Challenge. *Journal of the American Chemical Society, 141*(37), 14463–14479.
Greis, K., Mucha, E., Lettow, M., Thomas, D. A., Kirschbaum, C., Moon, S., … Pagel, K. (2020). The Impact of Leaving Group Anomericity on the Structure of Glycosyl Cations of Protected Galactosides. *Chemphyschem, 21*(17), 1905–1907.
Griffiths, P. R. (2017). The Early Days of Commercial FT-IR Spectrometry: A Personal Perspective. *Applied Spectroscopy, 71*(3), 329–340.
Guo, Q., Ai, L., & Cui, S. W. (2018). Strategies for Structural Characterization of Polysaccharides. In Q. Guo, L. Ai, & S. W. Cui (Eds.), *Methodology for Structural Analysis of Polysaccharides* (pp. 1–7). Berlin: Springer.
Han, Z., Shi, R., & Sun, D.-W. (2020). Effects of novel physical processing techniques on the multi-structures of starch. *Trends in Food Science & Technology, 97*, 126–135.
Hajji, M., Hamdi, M., Sellimi, S., Ksouda, G., Laouer, H., Li, S., & Nasri, M. (2019). Structural characterization, antioxidant and antibacterial activities of a novel polysaccharide from Periploca laevigata root barks. *Carbohydrate Polymers, 206*, 380–388.
Hayakawa, D., Nishiyama, Y., Mazeau, K., & Ueda, K. (2017). Evaluation of hydrogen bond networks in cellulose I beta and II crystals using density functional theory and Car-Parrinello molecular dynamics. *Carbohydrate Research, 449*, 103–113.
Hofmann, J., Hahm, H. S., Seeberger, P. H., & Pagel, K. (2015). Identification of carbohydrate anomers using ion mobility–mass spectrometry. *Nature, 526*(7572), 241–244.
Huang, W., Nie, Y., Zhu, N., Yang, Y., Zhu, C., Ji, M., … Chen, K. (2020). Hybrid Label-Free Molecular Microscopies for Simultaneous Visualization of Changes in Cell Wall Polysaccharides of Peach at Single- and Multiple-Cell Levels during Postharvest Storage. *Cells, 9*(3), 761. https://doi.org/10.3390/cells9030761
Hurtubise, F. G., & Krassig, H. (1960). Classification of Fine Structural Characteristics in Cellulose by Infared Spectroscopy. Use of Potassium Bromide Pellet Technique. *Analytical Chemistry, 32*(2), 177–181.
Jaravel, L., Schindler, B., Randon, J., Compagnon, I., Demesmay, C., & Dugas, V. (2020). Off-line coupling of capillary isotachophoresis separation to IRMPD spectroscopy for glycosaminoglycans analysis: Application to the chondroitin sulfate disaccharides model solutes. *Journal of Chromatography A, 1617*, 460782. https://doi.org/10.1016/j.chroma.2019.460782
Jiang, L., Wang, W., Wen, P., Shen, M., Li, H., Ren, Y., … Xie, J. (2020). Two water-soluble polysaccharides from mung bean skin: Physicochemical characterization, antioxidant and antibacterial activities. *Food Hydrocolloids, 100*, 105412. https://doi.org/10.1016/j.foodhyd.2019.105412
KASAAI, M. (2008). A review of several reported procedures to determine the degree of N-acetylation for chitin and chitosan using infrared spectroscopy. *Carbohydrate Polymers, 71*(4), 497–508.
Kazachenko, A. S., Tomilin, F. N., Pozdnyakova, A. A., Vasilyeva, N. Y., Malyar, Y. N., Kuznetsova, S. A., & Avramov, P. V. (2020). Theoretical DFT interpretation of infrared spectra of biologically active arabinogalactan sulphated derivatives. *Chemical Papers, 74*(11), 4103–4113.
Khanal, N., Masellis, C., Kamrath, M. Z., Clemmer, D. E., & Rizzo, T. R. (2017). Glycosaminoglycan Analysis by Cryogenic Messenger-Tagging IR Spectroscopy Combined with IMS-MS. *Analytical Chemistry, 89*(14), 7601–7606.
Khanal, N., Masellis, C., Kamrath, M. Z., Clemmer, D. E., & Rizzo, T. R. (2018). Cryogenic IR spectroscopy combined with ion mobility spectrometry for the analysis of human milk oligosaccharides. *Analyst, 143*(8), 1846–1852.
Kim, H. J., Liu, Y., French, A. D., Lee, C. M., & Kim, S. H. (2018). Comparison and validation of Fourier transform infrared spectroscopic methods for monitoring secondary cell wall cellulose from cotton fibers. *Cellulose, 25*(1), 49–64.
Korva, H., Kärkkäinen, J., Lappalainen, K., & Lajunen, M. (2016). Spectroscopic study of natural and synthetic polysaccharide sulfate structures. *Starch-Starke, 68*(9-10), 854–863.
Kruer-Zerhusen, N., Cantero-Tubilla, B., & Wilson, D. B. (2018). Characterization of cellulose crystallinity after enzymatic treatment using Fourier transform infrared spectroscopy (FTIR). *Cellulose, 25*(1), 37–48.
Kubicki, J. D., Mohamed, M. N. A., & Watts, H. D. (2013). Quantum mechanical modeling of the structures, energetics and spectral properties of I alpha and I beta cellulose. *Cellulose, 20*(1), 9–23.
Kubicki, J. D., Watts, H. D., Zhao, Z., & Zhong, L. H. (2014). Quantum mechanical calculations on cellulose-water interactions: Structures, energetics, vibrational frequencies and NMR chemical shifts for surfaces of I alpha and I beta cellulose. *Cellulose, 21*(2), 909–926.
Kubicki, J. D., Yang, H., & Kim, S. H. (2019). Integrating Density Functional Theory Calculations with Vibrational and Nuclear Magnetic Resonance Spectroscopy. In M. D. Smiths (Ed.), *Understanding Lignocellulose: Synergistic Computational and Analytic Methods* (pp. 89–102). Washington, DC: American Chemical Society.
Kumar, S., Lahlali, R., Liu, X., & Karunakaran, C. (2016). Infrared spectroscopy combined with imaging: A new developing analytical tool in health and plant science. *Applied Spectroscopy Reviews, 51*(6), 466–483.
Kyomugasho, C., Christiaens, S., Shpigelman, A., Van Loey, A. M., & Hendrickx, M. E. (2015). FT-IR spectroscopy, a reliable method for routine analysis of the degree of methylesterification of pectin in different fruit- and vegetable-based matrices. *Food Chemistry, 176*, 82–90.
Lee, C. M., Mittal, A., Barnette, A. L., Kafle, K., Park, Y. B., Shin, H., … Kim, S. H. (2013). Cellulose polymorphism study with sum-frequency-generation (SFG) vibration spectroscopy: Identification of exocyclic CH2OH conformation and chain orientation. *Cellulose, 20*(3), 991–1000.

Lettow, M., Grabarics, M., Mucha, E., Thomas, D. A., Polewski, Ł., Freyse, J., … Pagel, K. (2020). IR action spectroscopy of glycosaminoglycan oligosaccharides. *Analytical and Bioanalytical Chemistry, 412*(3), 533–537.

Lettow, M., Mucha, E., Manz, C., Thomas, D. A., Marianski, M., Meijer, G., … Pagel, K. (2019). The role of the mobile proton in fucose migration. *Analytical and Bioanalytical Chemistry, 411*(19), 4637–4645.

Li, Q., Wang, W., Zhu, Y., Chen, Y., Zhang, W., Yu, P., … Wu, X. (2017). Structural elucidation and antioxidant activity a novel Se-polysaccharide from Se-enriched Grifola frondosa. *Carbohydrate Polymers, 161*, 42–52.

Li, W., Cai, G., & Zhang, P. (2019). A simple and rapid Fourier transform infrared method for the determination of the degree of acetyl substitution of cellulose nanocrystals. *Journal of Materials Science, 54*(10), 8047–8056.

Li, X. L., Wei, Y. Z., Xu, J., Xu, N., & He, Y. (2018). Quantitative visualization of lignocellulose components in transverse sections of moso bamboo based on FTIR macro- and micro-spectroscopy coupled with chemometrics. *Biotechnology for Biofuels, 11*(1), 1–6.

Liu, J., Chen, J., Dong, N., Ming, J., & Zhao, G. (2012). Determination of degree of substitution of carboxymethyl starch by Fourier transform mid-infrared spectroscopy coupled with partial least squares. *Food Chemistry, 132*(4), 2224–2230.

Liu, M., Fu, L., Jia, X., Wang, J., Yang, X., Xia, B., … Guo, S. (2019). Dataset of the infrared spectrometry, gas chromatography-mass spectrometry analysis and nuclear magnetic resonance spectroscopy of the polysaccharides from C. militaris. *Data in Brief, 25*, 104126. https://doi.org/10.1016/j.dib.2019.104126

Liu, X., Renard, C. M. G. C., Bureau, S., & Le Bourvellec, C. (2021). Revisiting the contribution of ATR-FTIR spectroscopy to characterize plant cell wall polysaccharides. *Carbohydrate Polymers, 262*, 117935. https://doi.org/10.1016/j.carbpol.2021.117935

Liu, Y., Thibodeaux, D., Gamble, G., Bauer, P., & VanDerveer, D. (2012). Comparative Investigation of Fourier Transform Infrared (FT-IR) Spectroscopy and X-ray Diffraction (XRD) in the Determination of Cotton Fiber Crystallinity. *Applied Spectroscopy, 66*(8), 983–986.

Lucas, A. J. D., Oreste, E. Q., Costa, H. L. G., Lopez, H. M., Saad, C. D. M., & Prentice, C. (2021). Extraction, physicochemical characterization, and morphological properties of chitin and chitosan from cuticles of edible insects. *Food Chemistry, 343*, Article 128550.

Luo, M., Zhang, X., Wu, J., & Zhao, J. (2021). Modifications of polysaccharide-based biomaterials under structure-property relationship for biomedical applications. *Carbohydrate Polymers, 266*, 118097. https://doi.org/10.1016/j.carbpol.2021.118097

Makarem, M., Lee, C. M., Kafle, K., Huang, S., Chae, I., Yang, H., … Kim, S. H. (2019). Probing cellulose structures with vibrational spectroscopy. *Cellulose, 26*(1), 35–79.

Manrique, G. D., & Lajolo, F. M. (2002). FT-IR spectroscopy as a tool for measuring degree of methyl esterification in pectins isolated from ripening papaya fruit. *Postharvest Biology and Technology, 25*(1), 99–107.

Masellis, C., Khanal, N., Kamrath, M. Z., Clemmer, D. E., & Rizzo, T. R. (2017). Cryogenic Vibrational Spectroscopy Provides Unique Fingerprints for Glycan Identification. *Journal of the American Society for Mass Spectrometry, 28*(10), 2217–2222.

Molaei, H., & Jahanbin, K. (2018). Structural features of a new water-soluble polysaccharide from the gum exudates of Amygdalus scoparia Spach (Zedo gum). *Carbohydrate Polymers, 182*, 98–105.

Monsoor, M. A., Kalapathy, U., & Proctor, A. (2001). Improved Method for Determination of Pectin Degree of Esterification by Diffuse Reflectance Fourier Transform Infrared Spectroscopy. *Journal of Agricultural and Food Chemistry, 49*(6), 2756–2760.

Mucha, E., GonzálezFlórez, A. I., Marianski, M., Thomas, D. A., Hoffmann, W., Struwe, W. B., … Pagel, K. (2017). Glycan Fingerprinting via Cold-Ion Infrared Spectroscopy. *Angewandte Chemie-International Edition, 56*(37), 11248–11251.

Mucha, E., Lettow, M., Marianski, M., Thomas, D. A., Struwe, W. B., Harvey, D. J., … Pagel, K. (2018). Fucose Migration in Intact Protonated Glycan Ions: A Universal Phenomenon in Mass Spectrometry. *Angewandte Chemie-International Edition, 57*(25), 7440–7443.

Nada, A.-A., Kamel, S., & El-Sakhawy, M. (2000). Thermal behaviour and infrared spectroscopy of cellulose carbamates. *Polymer Degradation and Stability, 70*(3), 347–355.

Nasrollahzadeh, M., Sajjadi, M., Iravani, S., & Varma, R. S. (2021). Starch, cellulose, pectin, gum, alginate, chitin and chitosan derived (nano) materials for sustainable water treatment: A review. *Carbohydrate Polymers, 251*, 116986. https://doi.org/10.1016/j.carbpol.2020.116986

Nelson, M. L., & Oconnor, R. T. (1964). Relation of certain infrared bands to cellulose crystallinity and crystal latticed type. Part I. Spectra of lattice types I, II, III and of amorphous cellulose. *Journal of Applied Polymer Science, 8*(3), 1311–1324.

Nikonenko, N. A., Buslov, D. K., Sushko, N. I., & Zhbankov, R. G. (2005). Spectroscopic manifestation of stretching vibrations of glycosidic linkage in polysaccharides. *Journal of Molecular Structure, 752*(1-3), 20–24.

Pasandide, B., Khodaiyan, F., Mousavi, Z. E., & Hosseini, S. S. (2017). Optimization of aqueous pectin extraction from Citrus medica peel. *Carbohydrate Polymers, 178*, 27–33.

Pellegrinelli, R. P., Yue, L., Carrascosa, E., Warnke, S., Ben Faleh, A., & Rizzo, T. R. (2020). How General Is Anomeric Retention during Collision-Induced Dissociation of Glycans? *Journal of the American Chemical Society, 142*(13), 5948–5951.

Plata, M. R., Koch, C., Wechselberger, P., Herwig, C., & Lendl, B. (2013). Determination of carbohydrates present in Saccharomyces cerevisiae using mid-infrared spectroscopy and partial least squares regression. *Analytical and Bioanalytical Chemistry, 405*(25), 8241–8250.

Pozo, C., Rodriguez-Llamazares, S., Bouza, R., Barral, L., Castano, J., Muller, N., & Restrepo, I. (2018). Study of the structural order of native starch granules using combined FTIR and XRD analysis. *Journal of Polymer Research, 25*(12), 1–8.

Ray, B., Schutz, M., Mukherjee, S., Jana, S., Ray, S., & Marschall, M. (2021). Exploiting the Amazing Diversity of Natural Source-Derived Polysaccharides: Modern Procedures of Isolation, Engineering, and Optimization of Antiviral Activities. *Polymers, 13*(1).

Reiniati, I., Hrymak, A. N., & Margaritis, A. (2017). Recent developments in the production and applications of bacterial cellulose fibers and nanocrystals. *Critical Reviews in Biotechnology, 37*(4), 510–524.

Renois-Predelus, G., Schindler, B., & Compagnon, I. (2018). Analysis of Sulfate Patterns in Glycosaminoglycan Oligosaccharides by MSn Coupled to Infrared Ion Spectroscopy: The Case of GalNAc4S and GalNAc6S. *Journal of the American Society for Mass Spectrometry, 29*(6), 1242–1249.

Rongpipi, S., Ye, D., Gomez, E. D., & Gomez, E. W. (2019). Progress and Opportunities in the Characterization of Cellulose - An Important Regulator of Cell Wall Growth and Mechanics. *Frontiers in Plant Science, 9*, 1894.

Sahragard, N., & Jahanbin, K. (2017). Structural elucidation of the main water-soluble polysaccharide from Rubus anatolicus roots. *Carbohydrate Polymers, 175*, 610–617.

Schindler, B., Barnes, L., Gray, C. J., Chambert, S., Flitsch, S. L., Oomens, J., … Compagnon, I. (2017a). IRMPD spectroscopy sheds new (infrared) light on the sulfate pattern of carbohydrates. *The Journal of Physical Chemistry A, 121*(10), 2114–2120.

Schindler, B., Barnes, L., Renois, G., Gray, C., Chambert, S., Fort, S., … Compagnon, I. (2017b). Anomeric memory of the glycosidic bond upon fragmentation and its consequences for carbohydrate sequencing. *Nature communications, 8*(1). https://doi.org/10.1038/s41467-017-01179-y

Schindler, B., Joshi, J., Allouche, A.-R., Simon, D., Chambert, S., Brites, V., … Compagnon, I. (2014). Distinguishing isobaric phosphated and sulfated carbohydrates by coupling of mass spectrometry with gas phase vibrational spectroscopy. *Physical Chemistry Chemical Physics, 16*(40), 22131–22138.

Schindler, B., Laloy-Borgna, G., Barnes, L., Allouche, A.-R., Bouju, E., Dugas, V., … Compagnon, I. (2018). Online separation and identification of isomers using infrared multiple photon dissociation ion spectroscopy coupled to liquid chromatography: Application to the analysis of disaccharides regio-isomers and monosaccharide Anomers. *J Analytical chemistry, 90*(20), 11741–11745.

Schindler, B., Legentil, L., Allouche, A.-R., Ferrières, V., & Compagnon, I. (2019). Spectroscopic diagnostic for the ring-size of carbohydrates in the gas phase: Furanose and pyranose forms of GalNAc. *Physical Chemistry Chemical Physics, 21*(23), 12460–12467.

Schindler, B., Renois-Predelus, G., Bagdadi, N., Melizi, S., Barnes, L., Chambert, S., … Compagnon, I. (2017c). MS/IR, a new MS-based hyphenated method for analysis of hexuronic acid epimers in glycosaminoglycans. *Glycoconjugate Journal, 34*(3), 421–425.

Sevenou, O., Hill, S. E., Farhat, I. A., & Mitchell, J. R. (2002). Organisation of the external region of the starch granule as determined by infrared spectroscopy. *International Journal of Biological Macromolecules, 31*(1-3), 79–85.

Shi, X.-D., Nie, S.-P., Yin, J.-Y., Que, Z.-Q., Zhang, L.-J., & Huang, X.-J. (2017). Polysaccharide from leaf skin of Aloe barbadensis Miller: Part I. Extraction, fractionation, physicochemical properties and structural characterization. *Food Hydrocolloids, 73*, 176–183.

Smith, B. C. (2011). *Fundamentals of Fourier transform infrared spectroscopy* (2nd ed.). Boca Raton: CRC Press (Chapter 1).

Stefke, B., Windeisen, E., Schwanninger, M., & Hinterstoisser, B. (2008). Determination of the Weight Percentage Gain and of the Acetyl Group Content of Acetylated Wood by Means of Different Infrared Spectroscopic Methods. *Analytical Chemistry, 80*(4), 1272–1279.

Sugiyama, J., Persson, J., & Chanzy, H. (1991). Combined infrared and electron diffraction study of the polymorphism of native celluloses. *Macromolecules, 24*(9), 2461–2466.

Sun, Y., Wu, Z., Hu, B., Wang, W., Ye, H., Sun, Y.i., … Zeng, X. (2014). A new method for determining the relative crystallinity of chickpea starch by Fourier-transform infrared spectroscopy. *Carbohydrate Polymers, 108*, 153–158.

Szymanska-Chargot, M., Chylinska, M., Kruk, B., & Zdunek, A. (2015). Combining FT-IR spectroscopy and multivariate analysis for qualitative and quantitative analysis of the cell wall composition changes during apples development. *Carbohydrate Polymers, 115*, 93–103.

Tasumi, M. (2014). *Introduction to experimental infrared spectroscopy: Fundamentals and practical methods*. John Wiley & Sons.

Theis, T. V., Queiroz Santos, V. A., Appelt, P., M. Barbosa-Dekker, A., Vetvicka, V., F. H. Dekker, R., & A. Cunha, M. A. (2019). Fungal Exocellular (1–6)-β-d-glucan: Carboxymethylation, Characterization, and Antioxidant Activity. *International Journal of Molecular Sciences, 20*(9), 2337. https://doi.org/10.3390/ijms20092337

Thompson, J. M. (2018). *Infrared Spectroscopy* (1st ed.). Sinapore: Pan Stanford (Chapter 1).

Tribulová, T., Kačík, F., Evtuguin, D. V., Čabalová, I., & Ďurkovič, J. (2019). The effects of transition metal sulfates on cellulose crystallinity during accelerated ageing of silver fir wood. *Cellulose, 26*(4), 2625–2638.

Türker-Kaya, S., & Huck, W. C. (2017). A Review of Mid-Infrared and Near-Infrared Imaging: Principles, Concepts and Applications in Plant Tissue Analysis. *Molecules, 22*(1), 168.

Wan, Y.-J., Hong, T., Shi, H.-F., Yin, J.-Y., Koev, T., Nie, S.-P., Gilbert, R. G., & Xie, M.-Y. (2021). Probiotic fermentation modifies the structures of pectic polysaccharides from carrot pulp. *Carbohydrate Polymers, 251*, 117116. https://doi.org/10.1016/j.carbpol.2020.117116

Wang, Y.-X., Xin, Y., Yin, J.-Y., Huang, X.-J., Wang, J.-Q., Hu, J.-L., Geng, F., & Nie, S.-P. (2022). Revealing the architecture and solution properties of polysaccharide fractions from Macrolepiota albuminosa (Berk.) Pegler. *Food Chemistry, 368*, 130772. https://doi.org/10.1016/j.foodchem.2021.130772

Wang, J., Wang, Y., Xu, L.u., Wu, Q., Wang, Q.i., Kong, W., … Zhang, J.i. (2018). Synthesis and structural features of phosphorylated Artemisia sphaerocephala polysaccharide. *Carbohydrate Polymers, 181*, 19–26.

Wang, S., Xu, H., & Luan, H. (2020). Multiscale Structures of Starch Granules. In S. Wang (Ed.), *Starch Structure, Functionality and Application in Foods* (pp. 41–55). Singapore: Springer Singapore.

Wang, Y., Liu, Y., Yu, H., Zhou, S., Zhang, Z., Wu, D.i., … Zhang, J. (2017). Structural characterization and immuno-enhancing activity of a highly branched water-soluble β-glucan from the spores of Ganoderma lucidum. *Carbohydrate Polymers, 167*, 337–344.

Warnke, S., Ben Faleh, A., Scutelnic, V., Rizzo, T. R., et al. (2019). Separation and Identification of Glycan Anomers Using Ultrahigh-Resolution Ion-Mobility Spectrometry and Cryogenic Ion Spectroscopy. *Journal of the American Society for Mass Spectrometry, 30*(11), 2204–2211. https://doi.org/10.1007/s13361-019-02333-0

Warren, F. J., Gidley, M. J., & Flanagan, B. M. (2016). Infrared spectroscopy as a tool to characterise starch ordered structure-a joint FTIR-ATR, NMR, XRD and DSC study. *Carbohydrate Polymers, 139*, 35–42.

Wattjes, J., Schindler, B., Trombotto, S., David, L., Moerschbacher, B. M., & Compagnon, I. (2017). Discrimination of patterns of N-acetylation in chitooligosaccharides by gas phase IR spectroscopy integrated to mass spectrometry. *Pure and Applied Chemistry, 89*(9), 1349–1357.

Wellner, N. (2013). Fourier transform infrared (FTIR) and Raman microscopy: Principles and applications to food microstructures. In V. J. Morris, & K. Groves (Eds.), *Food Microstructures: Microscopy, Measurement and Modelling* (pp. 163–191). Cambridge: Woodhead Publishing Ltd.

Wiercigroch, E., Szafraniec, E., Czamara, K., Pacia, M. Z., Majzner, K., Kochan, K., … Malek, K. (2017). Raman and infrared spectroscopy of carbohydrates: A review. *Spectrochim Acta A Mol Biomol Spectrosc, 185*, 317–335.

Wu, A. C., Witt, T., & Gilbert, R. G. (2013). Characterization Methods for Starch-Based Materials: State of the Art and Perspectives. *Australian Journal of Chemistry, 66*(12), 1550–1563.

Wu, Y., Huang, Z., Chen, Y., Chen, N., & Liu, D. (2019). Recent applications of infrared (IR) and Raman chemical imaging in plant materials. *Applied Spectroscopy Reviews, 54*(1), 45–56.

Xiao, N., Bock, P., Antreich, S. J., Staedler, Y. M., Schönenberger, J., & Gierlinger, N. (2020). From the Soft to the Hard: Changes in Microchemistry During Cell Wall Maturation of Walnut Shells. *Frontiers in Plant Science, 11*. https://doi.org/10.3389/fpls.2020.0046610.3389/fpls.2020.00466.s00110.3389/fpls.2020.00466.s00210.3389/fpls.2020.00466.s00310.3389/fpls.2020.00466.s00410.3389/fpls.2020.00466.s00510.3389/fpls.2020.00466.s006

Xu, Y., Liu, G., Yu, Z., Song, X., Li, X., Yang, Y.u., … Dai, J. (2016). Purification, characterization and antiglycation activity of a novel polysaccharide from black currant. *Food Chemistry, 199*, 694–701.

Yalovenko, N., Yatsyna, V., Bansal, P., AbiKhodr, A. H., & Rizzo, T. R. (2020). Analyzing glycans cleaved from a biotherapeutic protein using ultrahigh-resolution ion mobility spectrometry together with cryogenic ion spectroscopy. *Analyst, 145*(20), 6493–6499.

Yan, J., Han, Z., Qu, Y., Yao, C.i., Shen, D., Tai, G., … Zhou, Y. (2018). Structure elucidation and immunomodulatory activity of a β-glucan derived from the fruiting bodies of Amillariella mellea. *Food Chemistry, 240*, 534–543.

Yang, Z., Mei, J., Liu, Z., Huang, G., Huang, G., & Han, L. (2018). Visualization and Semiquantitative Study of the Distribution of Major Components in Wheat Straw in Mesoscopic Scale using Fourier Transform Infrared Microspectroscopic Imaging. *Analytical Chemistry, 90*(12), 7332–7340.

Zhang, L., Hu, Y.u., Duan, X., Tang, T., Shen, Y., Hu, B., … Liu, Y. (2018). Characterization and antioxidant activities of polysaccharides from thirteen boletus mushrooms. *International Journal of Biological Macromolecules, 113*, 1–7.

Zhao, D., Yang, F., Dai, Y.a., Tao, F., Shen, Y.i., Duan, W., … Li, J. (2017). Exploring crystalline structural variations of cellulose during pulp beating of tobacco stems. *Carbohydrate Polymers, 174*, 146–153.

Zhao, M., Garcia-Vaquero, M., Przyborska, J., Sivagnanam, S. P., & Tiwari, B. (2021). The development of analytical methods for the purity determination of fucoidan extracted from brown seaweed species. *International Journal of Biological Macromolecules, 173*, 90–98.

Zhao, Y., Man, Y.i., Wen, J., Guo, Y., & Lin, J. (2019). Advances in Imaging Plant Cell Walls. *Trends in Plant Science, 24*(9), 867–878.

Zhi, F., Yang, T.-L., Wang, Q., Jiang, B., Wang, Z.-P., Zhang, J., & Chen, Y.-Z. (2019). Isolation, structure and activity of a novel water-soluble polysaccharide from Dioscorea opposita Thunb. *International Journal of Biological Macromolecules, 133*, 1201–1209.

Zou, Y., Du, F., Hu, Q., & Wang, H. (2019). The structural characterization of a polysaccharide exhibiting antitumor effect from Pholiota adiposa mycelia. *Scientific Reports, 9*(1), 1724.